



Invited review paper

Progress in developing spray-drying methods for the production of controlled morphology particles: From the nanometer to submicrometer size ranges

Asep Bayu Dani Nandiyanto, Kikuo Okuyama*

Department of Chemical Engineering, Graduate School of Engineering, Hiroshima University, 1-4-1 Kagamiyama, Higashi Hiroshima 739-8527, Japan

ARTICLE INFO

Article history:

Received 16 July 2010

Accepted 23 September 2010

Available online 25 October 2010

Keywords:

Nanomaterial processing

Spray pyrolysis route

Functional nanostructure

Composite material

Morphological control of particle

ABSTRACT

Control of particle size and morphology has increasingly captured the attention of researchers for decades. The exploration of unique sizes and shapes as they relate to various properties has become a great quest for large field applications. To meet these demands, this review covers recent developments in particle processing. An aerosol-assisted self-assembly technique, with a spray-drying method as a representative of it, to create particles is thoroughly reviewed. Its popularity and its broad use in industry for producing particles are the main reason of this review; thus, elucidation of this method is important for the improvement of particle technology. A practical spray-drying method is described from the step-by-step process to the selection of apparatus types (merits and demerits). Elaboration of particle processing of several morphologies (sphere, doughnut, encapsulated, porous, hollow, and hairy) is discussed in terms of the selection of material types, the addition of supporting materials, and the change of process conditions. Controllable size is also discussed in terms of the adjustment of the droplet size, initial precursor concentration, and the addition of specific techniques. A comparison between a theoretical mechanism and current experimental results (over a 15-year period) are shown to clarify how particles with various sizes and morphologies are designed. This method must be considered an art rather than a science because of its advantages in creating wonderful and unique particle shapes. The performance of various particle morphologies is also demonstrated, which is essential for an understanding of the importance that shape can exert on practical use. Because the method outlined here can be broadly applied to the production of various types of functional materials, we believe that this report contributes new information to the field of chemical, material, environmental, and medical engineering.

© 2010 The Society of Powder Technology Japan. Published by Elsevier B.V. and The Society of Powder Technology Japan. All rights reserved.

1. Introduction

Recently, control of particle morphology has received a tremendous amount of attention [1]. The change of shapes has caused unprecedented chemical and physical properties that differ markedly from those of bulk or dense material [2]. Great potential for use in various applications could be achieved with morphological control: electronics, catalysts, drug carriers, sensors, pigments, and magnetic and optical materials, etc., [3].

Effective strategies to tailor nanomaterials reliably and predictably are important [4]. Interest in them has increased in the past decade, especially when there is a need to control for different characteristics, such as size distribution, crystallinity, composition, and purity. Efforts toward the functionalization, formulation, and production of morphology have focused on making them applicable in industry. Many alternative methods have been proposed to realize production of particles with a controllable morphology:

mechanical milling, precipitation, lyophilization, freeze-drying, spray-drying, pyrolysis, supercritical fluid, emulsion-based methods, and a simple combination of chemical-process synthesis. Achievement from the current suggested processes for the use in practical applications has been reported. Controllable particle size within the desired range is also possible under specific conditions. However, exceptions and significant difficulties associated with the above methods remain: (i) particle size distribution; (ii) inadequate powder dispersibility; (iii) insufficient process control; (iv) contamination; (v) high-cost processing; (vi) excessive heat production problems; (vii) complexity of the processes; (viii) loss of chemical activity; (ix) yield of the products; and, (x) scaling-up the process [5].

Among the above processes, an aerosol-assisted self-assembly technique has been the most promising [6]. When the principles of this technique are combined with a drying process, an effective method can be created – namely, the aerosol-assisted spray method [6]. This method efficiently produces dry powder from either a liquid or a slurry [2]. The advantages of this method are prospective for many applications. A very versatile process that is

* Corresponding author.

E-mail address: okuyama@hiroshima-u.ac.jp (K. Okuyama).

Nomenclature

Alphabetical symbol

a	power constants of precursor density
b	power constants of precursor surface tension
c	power constants of precursor viscosity
C_i	concentration of component i (g/L)
C_m	desired concentration of the main component in the dried particles
C_0	initial precursor concentration
d_p	size of component
d_{p1}	size of component 1
d_{p2}	size of component 2
D	diffusion quantity
D_c	diffusion coefficient of component (m^2/s)
D_d	droplet diameter (μm)
D_p	volume mean diameter of the final particle (μm)
k	diffusion correction factor
K_1	antoine constants
K_2	antoine constants
K_3	antoine constants.
K_B	Boltzmann's constant ($=1.38 \times 10^{23}$ J/K)
K_f	excitation equipment constants (i.e. centrifugal force, frequency, pressure, and carrier gas velocity; which depends on the type of atomizer)
m	antoine constants
M_i	molecular weight of component i

n	power constant of volumetric flow rate
P_e	dimensionless Péclet number (–)
Q	precursor volumetric flow rate (mL/min)
R_c	component size (m)
s	particle porosity
t	minimum residence time (s)
T	temperature (K)
T_b	boiling temperature (K)
T_G	minimum temperature process (K)
T_{wb}	wet bulb temperature (K)

Greek symbol

ε	porosity of the particle
κ	evaporation rate
ρ	liquid density (kg/m^3)
ρ_{app}	densified particle density
ρ_i	density of component i (kg/m^3)
ρ_p	particle density
τ_D	maximum droplet drying time
σ	surface tension
μ_c	viscosity of the solvent ($kg/m s$)
μ	liquid dynamic viscosity (cP)

compatible with various materials is the main promising merits. Particles with a high-purity product can be produced simply using an economical, a continuous way [7], and a rapid process [8]. Furthermore, this method produces particles with a spherical shape that are agglomeration-free and have a relatively monodispersed size, which is very useful for material processing.

The spray method is well-trusted in practical uses, which has been confirmed by its use in the manufacturing of dried food, fertilizers, oxide ceramics, and pharmaceuticals. A magnificent number of the uses of spray method have been reported, in which more than 15,000 industrial-size spray dryers are currently in operation. This number would approximately double if the use in pilot plants and laboratories was added to the calculation [9].

Several developments of the spray method have been reported with no limitations to a particular type of process: spray-pyrolysis, spray-drying, flame-spray, low-pressure, and electro-spray [3]. The principle for all these processes is almost the same. A starting solution is prepared usually by dissolving the metal component of an intended product in a solvent. The droplets, which are atomized from the starting solution, are introduced to the solvent evaporator. Evaporation of the solvent, diffusion of solute, drying, and precipitation may occur inside the furnace to form the final product. The reaction among reactants, and sometimes with surrounding gas, is dependent on the type of the initial solution [10].

Here, at this juncture, we presented a review of all recent developments in particle processing using aerosol-assisted self-assembly technique. We focus only on the spray-drying method as representative of this technique to fabricate particles with a controllable size and morphology (Fig. 1). In addition, while our research group has had a considerable amount of success in research on this topic [10], we will not limit our review to work from our own group; rather, our review will be highly comprehensive.

The spray-drying method is similar to other types of spray (e.g. spray pyrolysis, spray freeze drying, etc.), except for the type of precursor (usually colloidal particles or sols) and the fact that there is almost no available reaction during the drying process. The

ability to produce uniformly spherical particles from nano to micron sizes is one of the main advantages of this method. Other merit gained from this method is that when the suspension consists of colloidal nanoparticles (primary particles), the resulting particles are comprised of nanoparticles that form a nano-structured powder. Therefore, the spray-drying method may be suitable for consolidating nanoparticles into macroscopic compacts, and submicron spherical powders that have nanometer-scaled properties can be obtained. A suitable process can be adjusted using this method, in which a striking feature of the initial raw material (e.g. initial particle size, type of material, physical and chemical properties, and surface charge) and process conditions play an important role in producing various product shapes [11]. Although the current spray-drying method is known to create particles by managing several parameters, no comprehensive report has described and reviewed all processes used to prepare particles with specific morphologies. In fact, due to this excellent prospect, in order to construct and design particles with a controllable morphology, it is important to understand the mechanisms and the regulations of the initial raw material and process-condition parameters when using the spray-drying method.

An overview of the current research on particle processing with its ability to control size and morphology to suit certain applications is described in this paper, which is believed to be the first detailed review of particle design (control of size and morphology). The main text comprises five sections, with the last being a summary. Section 2 provides a definition of the spray-drying method for the production of particles. Section 3 discusses the techniques for controlling particle morphologies. The manipulation of factors (i.e. process conditions and addition of supporting components) to realize particles of varying morphologies is thoroughly explained. The support of current results (described in the nanoparticle analysis (i.e. an X-ray diffraction (XRD), a scanning electron microscope (SEM), and a transmission electron microscope (TEM))) are also added to confirm the effectiveness of the above factors in producing particles with specific shapes. Theoretical

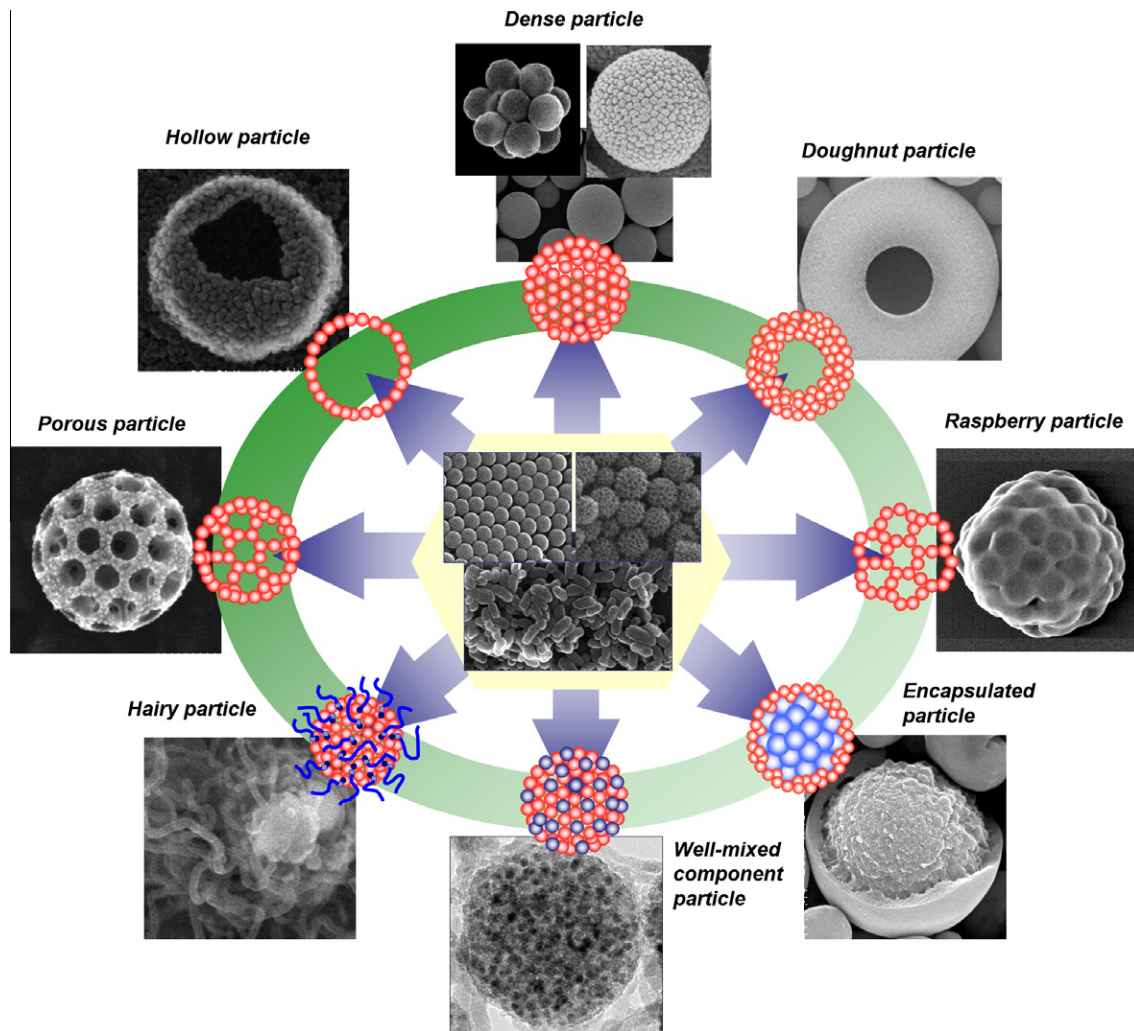


Fig. 1. Various particle morphologies prepared using the spray-drying method. Images were adapted and reprinted with permission from Refs. [29–32,36,43, and 45].

explanation, as well as mechanism illustration, is also described in this section to support and clarify the design of particles with various sizes and morphologies. Section 4 shows the effectiveness of various particle morphologies in several applications, which is important for understanding the significance of the effects of particle size and shape.

2. A spray-drying method: technical considerations for particle production

A representative of the spray-drying method is illustrated in Fig. 2. The main principle of this method is to deliver and rapidly heat an initial solution/slurry via the direct injection of very small droplets (Fig. 2a). The primary steps include atomization, droplet-to-particle conversion (solvent evaporation), and particle collection [3]. Details of the illustration apparatus of the spray-drying method, including atomizer, solvent evaporator, and particle collector types, are shown in Fig. 2b–d, respectively.

2.1. Atomization

Atomization is a key parameter in determining particle size. In this step, the initial liquid/slurry, namely a precursor, is fed into specific atomization equipment for conversion to droplet form. Accomplishment of this droplet formation task requires a specific technique. In the traditional method, aerosol generation via tem-

perature-assisted evaporation processing is typically used. The principle of this method is to produce droplet by vaporizing the precursor at a specific temperature (above the precursor temperature–evaporation level) [12]. Single and homogenous droplets can be produced using this method, but the cost of processing presents a problem. To address this shortcoming, the use of a specific driving force can be used as a substitution technique of traditional method. Several types of driving force can be employed to assist atomization process: pressure, centrifugal, electrostatic, and ultrasonic energy, which are selected depending on the required droplet size [13]. These driving forces can be installed in the spray method as an atomizer. In addition, several atomizers are available, such as a rotary disk, a two-fluid nozzle, and an ultrasonic nebulizer, which can produce droplets with a size of larger than 200; 10–1000; and, 1–10 μm , respectively [3].

In addition to the selection of an atomizer configuration, in order to control the size of droplets, the nature of the properties of the atomizing precursor (e.g., surface tension (σ), viscosity (μ), density (ρ), etc.) should be considered [14]. Control of droplet diameter (D_d), based on atomizer types and component properties, has been studied by many research groups. Empirical equation of control D_d can be expressed by the following equation [15]:

$$D_d = K_f \cdot Q^n [\rho^a \cdot \sigma^b \cdot \mu^c] \quad (1)$$

where K_f , Q , and n are the excitation equipment constants (i.e. centrifugal force, frequency, pressure, and carrier gas velocity; which

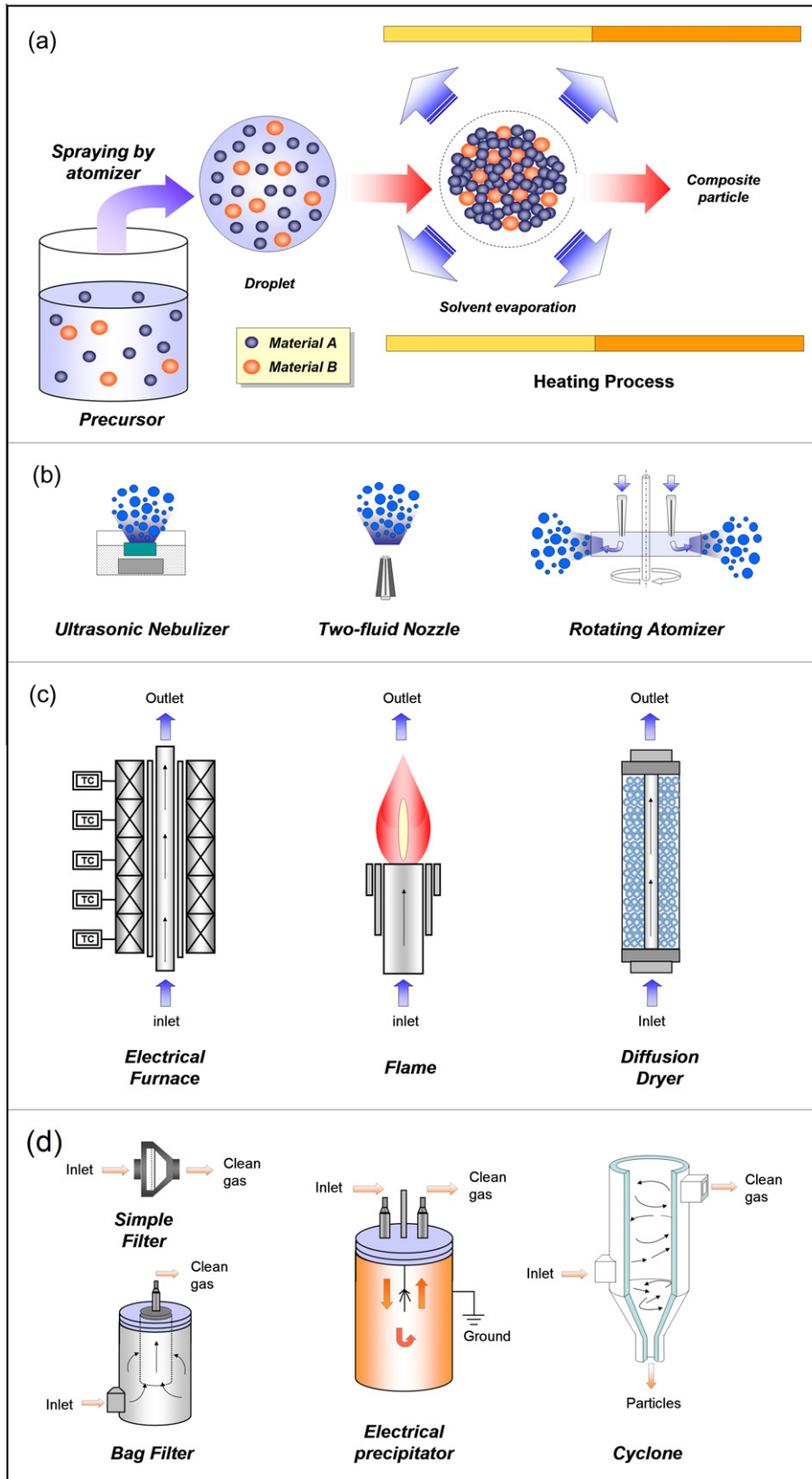


Fig. 2. Schematic illustration of nano-structured particle production using the spray-drying method and its apparatus: (a) mechanism; (b) atomizer; (c) solvent evaporator; and (d) particle collector.

Table 1
Power constants of some empirical atomizer models.

Atomizer types	Refs.	Power parameters			
		<i>n</i>	<i>a</i>	<i>b</i>	<i>c</i>
Air-shear nozzles	Lorenzetto and Lefebvre [82]	−1.93	−0.37	0.33	–
	Jasuja [83]	0.80	−0.40	0.45	0.80
	Hewitt [14]	0.10	–	2.40	−0.59
Spinning discs	Walton and Prewitt [84]	0.50	–	1.00	0.50
	Oyama et al. [85]	0.50	0.30	0.30	0.30
	Fraser et al. [86]	0.40	−0.30	0.30	0.10
	Ryley [87]	0.66	0.41	−0.88	−1.01
	Dombrowski and Lloyd [88]	1.55	0.93	1.22	0.22
	Kayano and Kamiya [89]	1.01	0.19	0.95	1.34
	Tanasawa et al. [90]	0.60	0.34	1.00	0.50
	Frost [91]	1.24	0.80	0.95	0.82
	Sanderson [14]*	0.33	0.15	0.15	0.15
	Kinnersley [14]*	0.88	0.72	0.72	0.72
	Hewitt [14]	0.20	–	–	–
Rotary cage atomizers	Parkin and Siddiqui [92]	0.85	0.68	0.68	0.68
	Hewitt (<i>N</i> < 5500) [14]	0.12	–	–	–
	Hewitt (<i>N</i> > 5500) [14]	0.03	–	1.62	0.26
Ultrasonic nebulizer	Lang [93]	–	−0.67	0.33	–
	Mochida [94]	0.14	−0.35	0.35	0.30
	Rajian and Pandit [95]	0.21	−0.27	0.11	0.17

Note: *value was a re-calculation from Hewitt et al. [14].

depends on the type of atomizer) [14], the precursor volumetric flow rate, and the power constant of volumetric flow rate, respectively. The symbols *a*, *b*, and *c* are, respectively, the power constants of precursor properties: the density, the surface tension, and the viscosity.

The power constants for the empirical atomization model are shown in Table 1. This table implies that generally, the droplet size generated from the atomizer is mostly proportional to the liquid flow rate, the surface tension, the density, and the viscosity of the precursor [15].

2.2. Droplet-to-particle conversion

Beside the atomization, the droplet-to-particle conversion cannot be neglected. This step is crucial for the removal of solvent from the generated droplets (produced by atomizer) and the transformation into particles. Principally, the droplets that are generated from the atomizer enter the droplet-to-particle conversion chamber via the flow of carrier gas. The aerosol droplets undergo evaporation and solute condensation within the droplet. This step results in the solvent removal, while the desired components remain in the final product (dried particles) [8]. Formation of particles with micro-porous structures (following a sintering process) occurs [16], resulting in the creation of compacted components. The carrier gas used to transport aerosol droplets into this chamber generally will be either air, inert gas (e.g. nitrogen, argon), hot gas, or steam, depending on the chemical component types [3].

One of three configurations of the droplet-to-particle conversion process can be selected: (i) solvent evaporation via heat treatment using a heated carrier gas [5], (ii) solvent evaporation via heat treatment using a hot furnace or a reactor [17], and (iii) solvent evaporation via a solvent-diffusion process using a diffusion drier [7]. The selection of the configuration depends on the component properties (e.g., bioactivity and thermal decomposition) [18]. In addition, among these types of droplet-to-particle conversion processes, the heat treatment is typically used as the solvent removal procedure.

A key to successful droplet-to-particle conversion using the heat treatment is optimizing the process conditions. This optimization can be achieved by managing the geometry of the chamber, the carrier gas flow rate, the pressure, and the temperature process

[3]. To achieve this key point, principle of heat and mass transport phenomena must be understood. The heating process must be controlled at a specific temperature to make sure that the solvent is removed completely from the droplet. The minimum temperature process (*T_c*) can be empirically approximated using a simple Antoine equation [19]:

$$T_{wb} = K_1 \left(\frac{T_b}{K_2} \right)^m \log(T_c) + K_3 \quad (2)$$

where *T_{wb}* and *T_b* are the wet bulb and the boiling temperature, respectively. The symbols *K₁*, *K₂*, *K₃*, and *m* are the Antoine constants.

The characteristic temperature given above is useful for the droplet-to-particle formation step. Selection of temperature can be estimated using the above equation to make a complete solvent evaporation. However, the optimization of the process depends not only on temperature. Calculation of residence time is also required to ensure the process has sufficient drying time [8]. The minimum residence time (*t*) can be calculated using a simple mass balance in the spraying process [20]:

$$C_m = C_0 \left(1 - \frac{t}{\tau_D} \right)^{-\frac{3}{2}} \quad (3)$$

where *C_m*, *C₀*, and *τ_D* are the desired concentration of the main component in the dried particles, the initial precursor concentration, and the maximum droplet drying time, respectively. The *C_m* is the final concentration of the required product after the spray-drying process. This concentration is relevant to the concentration of solvent remaining in the final product. The *τ_D* is also crucial for an estimation of the best drying time. This value can be estimated using the initial droplet diameter (*D_d*) and the evaporation rate (*κ*) [21,22]:

$$\tau_D = D_d^2 / \kappa \quad (4)$$

The prediction of *κ* must be integrated numerically to gain the exact number [23]. Typically, to simplify the calculation of this value, a dimensionless Péclet number (*P_e*) can be used [20] that is relevant to the physical properties and the diffusion quantity (*D*) of the droplet components:

$$P_e = \frac{\kappa}{8D} \quad (5)$$

Table 2
Practical use of particle collector [24,25].

Collector type	Efficient size of particles be captured (μm)	Collection efficiency (%)	Cost	
			Equipment	Processing
Gravity settling	>100	40–50	Small	Small
Filtration	<2	90–99	Medium to high	Medium to high
Wet scrubbing	>1	80–95	Medium	High
Cyclone	>5	85–95	Medium	Medium
Electrostatic precipitator	<10	90–99	High	Small to medium

2.3. Particle collection

After the droplet-to-particle step is finished, the solvent-free particles must be collected. Several pieces of equipment have been recommended, and can be chosen based on the material types, the mass of the products, and the particle sizes: a cyclone, a filter bag, or an electric field precipitator (Table 2) [24,25]. Details of the other methods for particle collection and the choice among methods are provided by Svarovsky [26,27] and Perry and Green [28].

3. Various particles morphologies

The spray-drying method has great potential for the synthesis of particles that are rich in desirable properties. A simple process can be achieved, which involves only solvent evaporation and self-assembly of materials inside the droplet system, as described above. The control of particle shape is also possible by adding some technical modifications. The features of the initial raw material (e.g., initial particle size, type of material, physical and chemical properties, and surface charge) and process conditions play an important role in producing various products [10,11,29]. Using this suitable process, a summary of research on particle processing via spray routes over a 15-year period (1995–2010) is shown in Table 3.

Examples of the aerosol spray-drying method for the preparation of spherical and doughnut-shaped particles, composite and microencapsulated particles, porous and hollow particles, and hairy particles are described, as follows:

3.1. Spherical, hollow, and doughnut-shaped particles

Fig. 3 shows the possibilities for controlling particle morphology using the spray-drying method. Various particle morphologies can be produced by changing the process conditions. The mechanism of the particle formation is illustrated in Fig. 3a. Spherical-shaped particles are typically generated using the spray method, which can be fabricated from either colloidal solution, sol nanoparticle, or alkoxide solution (Fig. 3a; R1). The maximum structural stability of the solution is in a spherical form, which is the fundamental reason for producing this shape [20]. However, the change of several parameters, which are related to the mass and the heat transfer of the droplet, can result in different particle morphologies [20]. The adjustment of mass [35] and heat transfer-related parameters [29] (i.e. characteristic time for solute to reach saturation (skin formation), heat transfer from the surface to the deepest point inside the droplet, and drying residence time) can create hollow particles (Fig. 3a; R2) [30]. A variation of the initial size of the precursor, when using nanoparticles as an alternative to a liquid precursor, can produce spherical particles with differing surface roughness (Fig. 3a; R3) [31]. The selection and the adjustment of the initial physicochemical properties of the droplet are also important, which is known as bond number correlation. Changes

in the hydrodynamics, the structural stability, and the behavior of the droplets can occur, allowing the transformation of a droplet from spherical, mushroom and convex, to a doughnut form (Fig. 3a; R4) [32]. In practice, this droplet-transformation phenomenon happens when there is a change in the specific parameters (i.e. viscosity, drying temperature, gas flow rate, and addition of surfactant), the type of spray injection, and the droplet-gas contact flow (i.e., co-current, counter-current, and mixed flow) [30–32,104].

To confirm the effectiveness of the above mechanism in fabricating particles with various morphologies, the SEM and the TEM analysis results are represented in Fig. 3b–g). Fig. 3b shows the spherical silica particles produced using the spray method. This figure confirms that under usual conditions, the spray method typically generates a spherical shape [30]. The adjustment of some parameters can produce particles with a unique morphology. The change of mass- and heat-transfer parameters caused the production of hollow particles (Fig. 3c and d), which was believed to be an effect of component movements in the droplet [35] and of a high evaporation rate [29]. Variation of the initial precursor parameters (i.e. nano-precursor size), which was performed under low-evaporation rate conditions to insure the preparation of dense particles, resulted in spherical particles with differing surface forms. The use of nanoparticles with the size of several nanometers allowed the production of small-roughness spheroidal particles (Fig. 3e) [30]. However, when the size of the nano-precursor was nearer the size of the droplet, the creation of particles consisting of only several spheres could be obtained (Fig. 3f) [31]. In other cases, the change of the process conditions that were related to the hydrodynamics, structural stability, and the behaviour of the droplets caused the formation of doughnut particles (Fig. 3g) [32].

3.2. Composite particles and their derivatives

Composite particles, which are defined as particles comprised of several components, have become one of the most attractive topics recently due to their useful in large field applications [3]. Studies on this composite (consisted of multi-component and structures) have been intensively reported. However, to simplify the description of composite particles, we focused only on the particle containing two components. One component acts as a main material, while the other is a supporting material. From the use of both components in the initial precursor, unique results can be obtained: (i) particles with well-distributed components, (ii) microencapsulated particles, and (iii) hairy particles.

3.2.1. Well-distributed components and microencapsulated particles

In conventional theory, when two components are mixed in the solvent and dried, the final material produced is a mixture of both components. The component domination in the final material depends on the fractions of the components in the initial precursor. This suggests an idea to control particle morphology by changing

Table 3
Various particle morphologies prepared via spray routes (1995–2010).

Morphology	Material type	Size (nm)	Precursor	Specific treatment	Refs.
Dense particle	Inorganic particles	>100	Nanoparticle sols (e.g. nano silica, nano boron nitride, nano titania, etc.)	–	[31,37,43,63]
		>200	Single solute precursor (e.g. TEOS, TiCl ₄ , TC-300, TC-400, TTIP)	–	[63,67]
			Multi Solute precursor (e.g. Gd nitrate + Y Nitrate + Eu; ZHA + YHA; CH ₃ COOLi + FeC ₂ O ₄ + (NH ₄) ₂ HPO ₄)	–	[96–98]
Doughnut particle	Silica	>500	Nano silica	–	[32]
	Aluminum	>500	Aluminum solution	–	[99]
	Hydroxyapatite (drugs)	>1000	Ca(NO ₃) ₂ + (NH ₄) ₂ HPO ₄ + NH ₃	–	[100]
Hollow particle	Clay	>1000	Sodium montmorillonite + alkylsulphonate	–	[101]
	Silica	>200	Phenolic resin + TEOS + Pluronic P123 + span 80 + vapor HCl	–	[102]
	TiO ₂	>700	TiO ₂ nano + silica nano	–	[1]
	ZrO ₂	>500	Zr(OH)Cl	–	[29]
			Zr(OH) ₂ (H ₂ O) ₄ Cl ₂	–	[103]
	Drugs	>1000	Drugs component + PSL	–	[78]
Microencapsulated particle	Inorganic/inorganic particles	>500	Nano silica + nano silica Zr(NO ₃) ₂ + nano silica Al(NO ₃) ₃ + nano silica	–	[36]
		>10,000	Inorganic salts ^a (sulfates; nitrates; acetates; carbonates; chlorides; organometallic salts)	–	[104]
	Food or drugs by organic compound	>500	Main component + organic compound (e.g. carbohydrate, dextrose, gums, gelatin, and protein)	–	[33,105,106]
Porous particle	TiO ₂	>400	Nano brookite + PSL	–	[17]
		>200	Nano anatase + PSL	–	[6]
		>100	TiCl ₄	–	[11]
	Silica	>100	Nano silica + PSL	–	[35,38,50,54]
		>100	TEOS + PSL	–	[11]
		>200	TEOS + surfactant ^b	–	[55,56][102]
		~1000	Nano silica + salt	–	[51]
		>1000	SiCl ₄ + metal carbonate	–	[107]
	Al ₂ O ₃	>500	Al(OH) ₃ + CTAB	–	[108]
		>100	Al(NO ₃) ₃ + PSL	–	[11]
	Aluminium organophosphonate	>1000	AlCl ₃ + pluronic	–	[52]
	Hyaluronic acid (drugs)	>1000	Hyaluronic acid + PSL	–	[5]
	Y ₂ O ₃	>200	Y(NO ₃) ₃ + PSL; Y(NO ₃) ₃ + PSL + Eu	–	[11,81]
Carbon	>1000	Alkali metal chloroacetate	–	[109]	
ZrO ₂	>200	ZrO(OH)Cl + PSL	–	[11]	
Hairy particle	CNT	Tubes from >10	Metallocenes + hydrocarbons	–	[40]
		Tubes from >10	Ferrocene + ethanol	–	[41]
	CNT/BN	>100	Nano BN + ferrocene Nano BN + CoPd	–	[43] [37]
	CNT/silica	>100	CNT + TEOS/TMOS	–	[42]
Nanoparticle	TiO ₂	>10	TTIP; TC-300; TC-400	LP	[67]
	Y ₂ O ₃	>10	Y(NO ₃) ₃ + Eu(NO ₃) ₃	LP	[110]
	CeO ₂	<20–120	Ce(NO ₃) ₄	LP	[66]
	ZrO ₂	<200	ZrO(OH)Cl + Salt	AS	[110]
	CeO ₂	25–100	Ce(NO ₃) ₄ + EG	AS	[111]
	BaSO ₄	4–8	Ba(OH) ₂ ·8H ₂ O + EG	AS	[53]
	CdSe	<10	Cd compound + Se compound + toluene ^c	AS	[65]
	Silica	10–75	Hexamethyldisiloxane	FS	[112]
	YAG:Ce	5–700	Y(NO ₃) ₃ + Al(NO ₃) ₃ + (Ce(NO ₃) ₃)	FS	[113]
	Y ₂ O ₃	30–700	Y(NO ₃) ₃	FS	[64]
	Bismuth	50–130	Bi(C ₈ H ₁₅ O ₂) ₃ + O ₂	FS	[61]
	Inorganic composite nanoparticles ^d	<100	Inorganic solution	FS	[69]

LP = low pressure-assisted spray method; AS = additive-assisted spray method; FS = flame-assisted spray method; TTIP = titanium tetra-isopropoxide; EG = ethylene glycol; TEOS = tetraethylorthosilicate; PSL = polystyrene spheres; YAG:Ce = Y₃Al₅O₁₂:Ce³⁺; ZHA = Zr(OH)_x(CH₃COO)₄ (x = 2.64); YAH = (CH₃COO)₃Y.

^a Reviewed in the book.

^b CTAB (cetyltrimethylammonium bromide), Brij-56 (CH₃(CH₂)₁₅(OCH₂CH₂)₁₀OH), or P123 ((CH₂–CH₂O)₂₀(CH₂(CH₃)CH₂O)₇₀(CH₂CH₂O)₂₀).

^c Cd component (CdO, CdCO₃, Cd naphthenate, and Cd(CH₃CO₂)₂) and Se component (Triethylphosphine selenide).

^d (V₂O₅/TiO₂, TiO₂/SiO₂, perovskites, Pt/TiO₂, Pd/Al₂O₃, Pt/CeO₂/ZrO₂, Pt/Ba/Al₂O₃, Ag/ZnO, Cu/ZnO/Al₂O₃, Pd/Pt/Al₂O₃, and Au/TiO₂).

the fractions of the components, e.g., the concentrations and the sizes of the components.

Fig. 4 shows the possibility of producing particles with well-distributed components and microencapsulated structures. The figure focuses on the effect of component size on particle morphol-

ogy, in which other parameters are assumed to be the same. Fig. 4a is an illustration of the simple mechanism of a particle formation consisting of two components. When the fraction of each component is the same, particles with a well-mixed component can be obtained (Fig. 4a; R1) [36,37]. However, when the fraction is

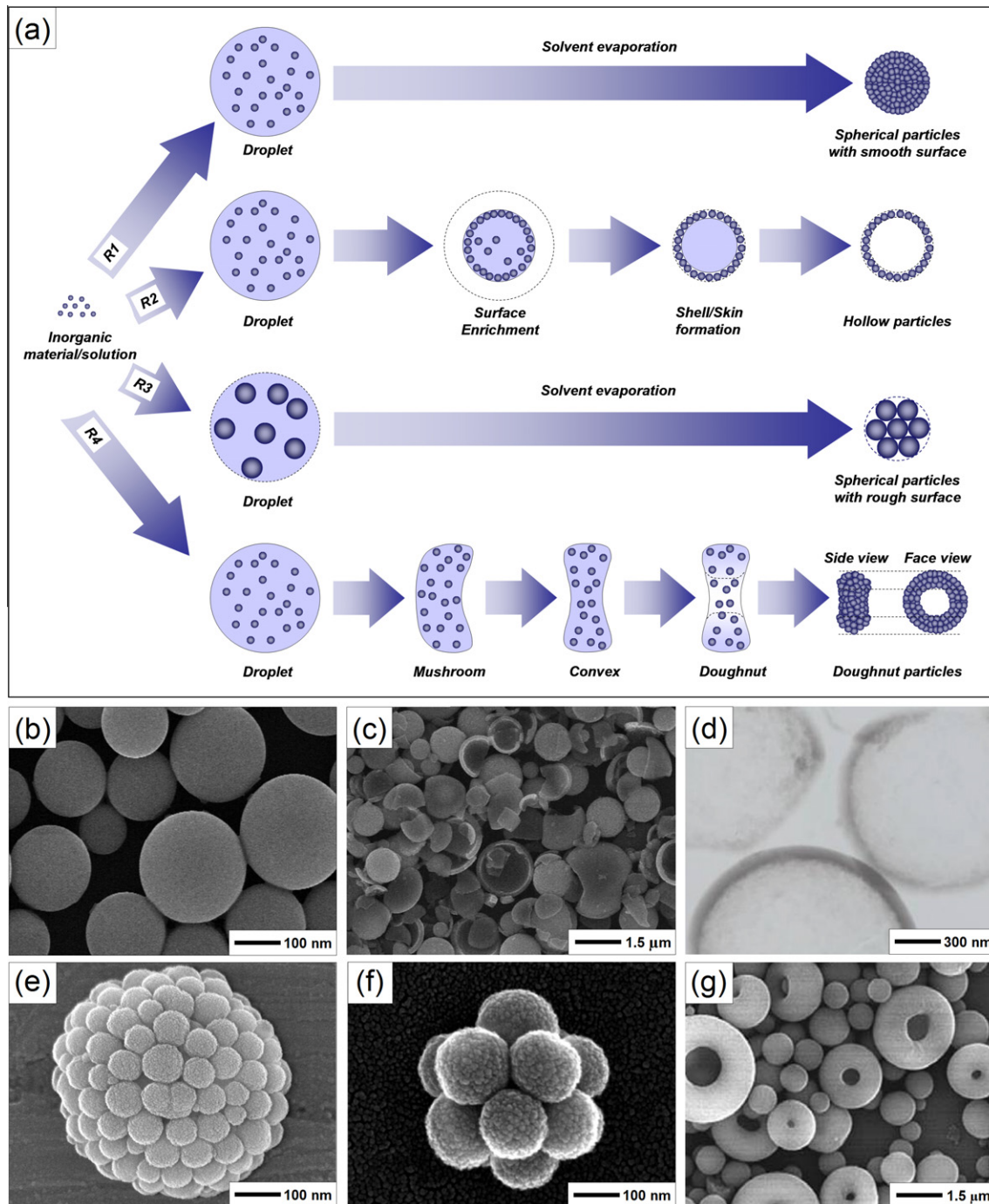


Fig. 3. Various particle morphologies: (a) formation mechanism; (b) spherical particles with smooth surface produced from alkoxide; (c) SEM image of broken hollow ZrO_2 particles; (d) TEM image of hollow ZrO_2 particles; (e) spherical particles prepared from silica nanoparticle 70 nm; (f) spherical particles prepared from silica nanoparticle 120 nm; and, (g) doughnut silica particles prepared by changing specific parameters. (c and d), (e and f), and (g) were reprinted with permission from Refs. [29],[31], and [32], respectively.

different, unique particles can be produced (Fig. 4a; R2). A surrounding or a coating of one component by others can be created, which is known as the microencapsulation phenomenon [33].

Diffusion plays an important part in these hypothesis phenomena. Different diffusion rates affect the particle movement in the droplet, which can be described by conventional calculation, as follows [9].

$$D_c = k \frac{K_B T}{6\pi\mu_c R_c} \quad (6)$$

where D_c , k , K_B , T , μ_c , and R_c are the diffusion coefficient of component (m^2/s), the diffusion correction factor, the Boltzmann's constant ($=1.38 \times 10^{-23} J/K$), the temperature (K), the viscosity of the solvent ($kg/m \cdot s$), and the component size (m), respectively. The diffusion coefficient has a correlation negative to the size of the component. Because the diffusion coefficient describes the particle movement rate [20], this equation suggests that the component movement increases along with a decrease in component size.

The simplification of this phenomenon can be described as follows. During solvent evaporation, a meniscus region is formed. The

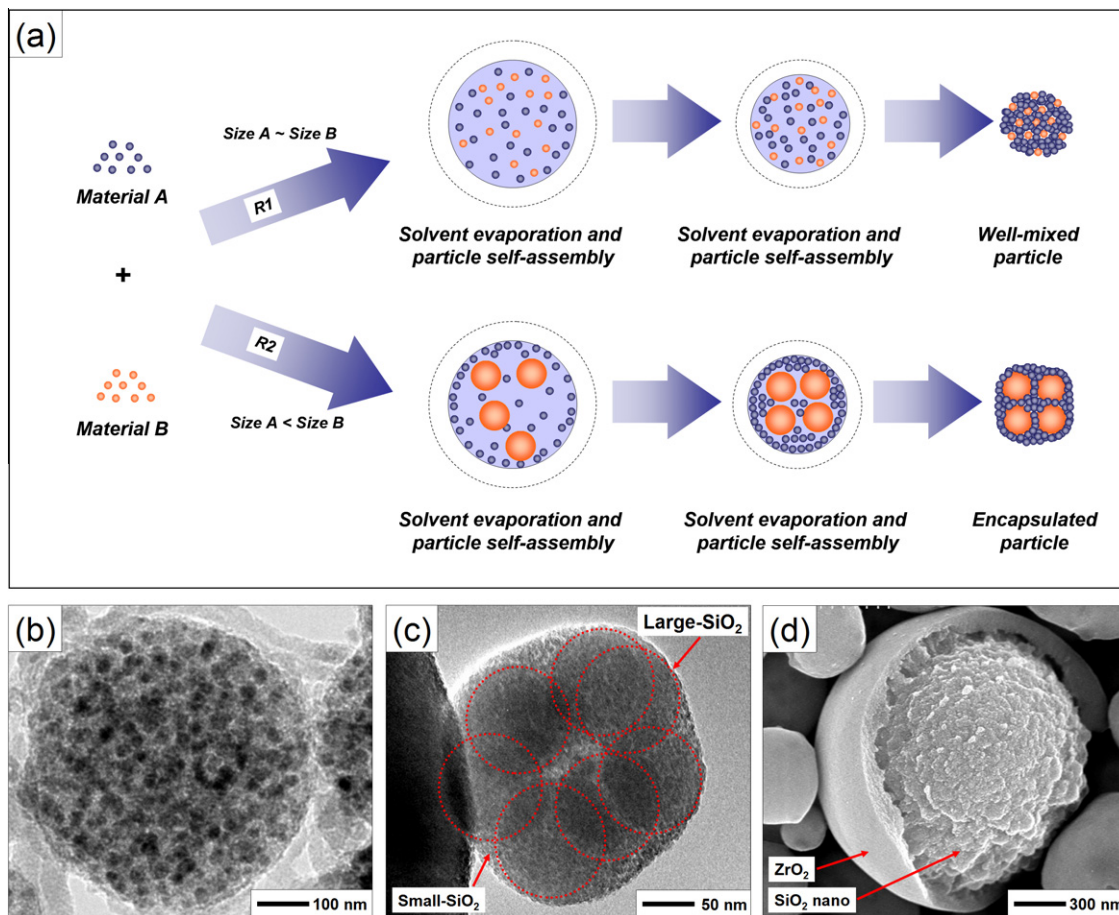


Fig. 4. Composite particles prepared by the spray-drying method: (a) mechanism; (b) well-dispersed particles; (c) microencapsulated particle using nanoparticle; (d) microencapsulated particles using alkoxide. (c and d) were reprinted with permission from Ref. [36].

meniscus region is the interface region where all of the solvent can no longer be held in its liquid phase, and some of the solvent begins to vaporize. Solvent evaporation from this meniscus region induces capillary flow, and the interparticle capillary forces cause self-assembly of the colloidal particles into the close-packed arrays. All components at the very beginning of the process are distributed homogeneously in the droplet. As a result of the buoyancy force, the components move to the meniscus region. When the component sizes are almost similar, a particle with a well-distributed component structure can be obtained due to equal component movement rates. However, when different fraction components (large and small particles) are interfered with, unique phenomena can occur. Smaller particles have a lower buoyancy force, but have a larger Brownian motion effect, than the large particles. For this reason, the smaller particles can easily move and swirl from one position to another [9]. This condition also permits the smaller particles to move and arrange faster to the meniscus region, while the large particles are slow but can easily shift the arrangement of smaller components in the interstitial channels between spheres [34]. Since the movement of the meniscus region is very fast, the small particles that exist in the meniscus region are trapped. The movement of particles in the meniscus region becomes very limited. The channels between trapped particles are jammed and filled by the interstitial small particles, which cause the discontinuity of flow entering the meniscus and the movement of configured particles [35]. Further, when the meniscus region passes the particle arrangements, no particle movement is possible. This condition makes it possible for a smaller component to

coat a larger component [36]. Detailed information about this mechanism is reported elsewhere [34,35].

Several examples for the above hypothesis are represented in Fig. 4b and d. The particles with well-mixed components, consisting of CoPd and BN, could be produced when 20 nm of CoPd nanoparticles and 30 nm of BN nanoparticles were mixed in the same ratio [37] (Fig. 4b). The component fractions (both volume (from the particle size calculation) and concentration) were equal, explaining the fundamental reason for the production of this type of particle. However, when different sizes of components (e.g. silica particles with size of 109 and 6 nm) were employed, microencapsulated particles were created (Fig. 4c). The confirmation results for the above hypothesis showed that the smaller particles were moved easily to the meniscus and formed an encapsulated film in the final particle surface. 109-nm silica particles had a tendency to be placed inside the droplet, while 6-nm silica nanoparticles had a tendency to move to the surface and to form a coating. Similar results were also observed for other cases consisting of different material types and sizes. For example, in the preparation of an $\text{Al}_2\text{O}_3/\text{SiO}_2$ powder from a mixture of Al_2O_3 (18 nm) and a SiO_2 (109 nm) sol precursor, Al_2O_3 particles appeared on the surface of the prepared powder while silica was placed inside the particles [36].

To confirm the above hypothesis in particle movement, the combination of nanoparticles and solute component is also presented in this review. Iskandar et al. reported the encapsulation of silica particles prepared from a mixture of SiO_2 sol (5 nm) and an aqueous precursor solution of zirconyl nitrate dehydrate

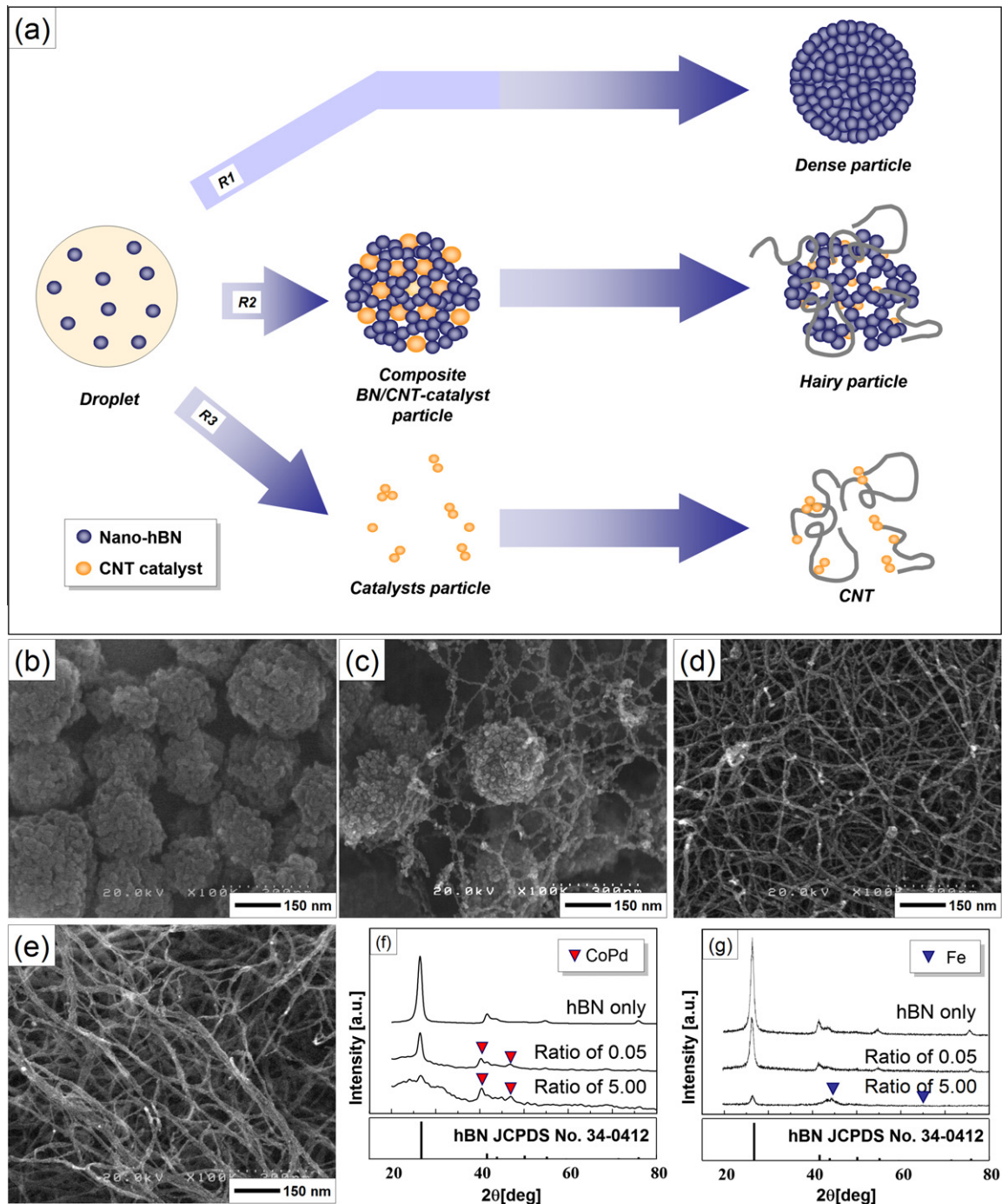


Fig. 5. Formation of composite BN/CNT particles: mechanism illustration (a); particle morphology preparation ((b) BN only; (c) additional catalyst in the initial precursor; (d) catalyst in the high concentration; (e) catalyst only); and XRD analysis of prepared BN/CNT catalyst ((f) using CoPd as catalyst; (g) using ferrocene as catalyst). (b–e) and (g) were reprinted with permission from Ref. [43], while (f) is from Ref. [37].

(Fig. 4d) [36]. The results verified that during the evaporation process, the solute component had a tendency to move to the surface of the droplet [20], while sol nanoparticles were relatively confined to deep inside the droplet. After the surface was dried, the solute components were reacted (e.g. zirconyl nitrate to zirconium) or dried, allowing the formation of a shell in the final product [36]. This procedure is limited not only to the preparation of inorganic particles but applies to all material types, as reported by Gharsallaoui et al. [33] and Vehring [20] in the coating of material by several organic components (e.g., carbohydrates, gums and proteins).

In addition to the effect of component size on the creation of microencapsulated particles, other parameters also should be considered; for instance, the charge of the particle is also crucial in forming particles using the microencapsulation phenomenon [38]. Detailed information concerning particle charge and other parameters will be described in a future study.

3.2.2. Hairy particles

Well-dispersed particle formation has been discussed in the above section. The formation of those particles can be obtained when almost identical amounts of each component are used. The

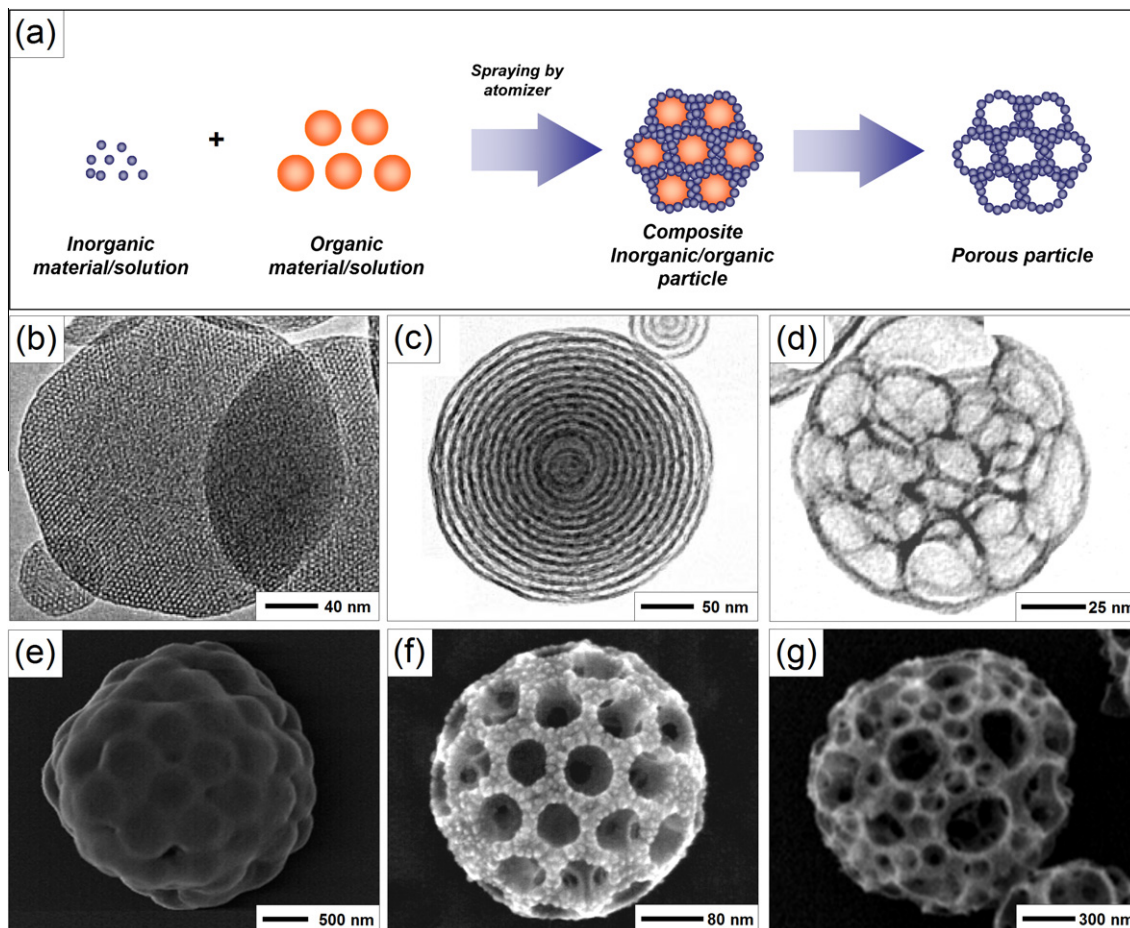


Fig. 6. Spray-dried porous particles produced from various templates: (a) mechanism illustration; (b) CTAB (cetyltrimethylammonium bromide); (c) P123 ($(\text{CH}_2\text{-CH}_2\text{O})_{20}(\text{CH}_2(\text{CH}_3)\text{CH}_2\text{O})_{70}(\text{CH}_2\text{CH}_2\text{O})_{20}$); (d) poly(propylene glycol dimethylacrylate) and 1,19 - azobis (1 - cyclohexanecarbonitrile); (e) polystyrene particles with positively zeta charge; (f and g) polystyrene particles with negatively zeta charge. SEM analysis (b–d), (g) and (f) were reprinted with permission from Refs. [30,31,35], respectively.

above particle formation phenomenon and hypothesis is important and very useful for further particle development in material processing. For example, the preparation of composite carbon nanotube (CNT) particles can be achieved by the above phenomenon, by adding CNT catalyst to the precursor. CNT formation is a focus of this review because CNT have been extensively studied in the past decade [39].

Vivekchand et al. reported the preparation of CNT using metal-locenes as the CNT catalyst and various hydrocarbons as the carbon source [40]. That procedure was then developed by Su et al., who prepared these materials using harmless chemicals and side products (e.g. CO) [41]. Further developments were reported by Iskandar et al. They reported a possibility for the fabrication of CNT composed with other composite materials [37], which is believed to be the first report of the synthesis of composite CNT/inorganic particles (namely, hairy particles) via an *in situ* process. A simple fabrication procedure was achieved. In short, to synthesize composite CNT particles, they used CoPd nanoparticles (as the CNT catalyst), BN nanoparticles (as the supporting material), and ethanol (as the solvent and the carbon source). The mixture was then spray-dried to produce composite BN/CNT particles in one step process. This preparation was different from other common CNT composite material preparation methods, in which the conventional procedure was typically complicated and required multistep process. Furthermore, this conventional procedure results in that CNT and other components are not composed chemically [42]. Other advantage from Iskandar et al., method is the possibility in

controlling CNT tube length, tube diameter, and population. As a continuation of the Iskandar method [37], Nandiyanto et al., from the same research group, reported the preparation of particles consisting of BN and CNT using the same method but with different types of catalysts [43]. Ferrocene was selected as a model solute catalyst, as it was more convenient for practical use because no catalyst nanoparticle synthesis steps were required.

Fig. 5 shows the composite CNT particle formation mechanism with analysis results. The mechanism in Fig. 5a describes the possibility of preparing composite CNT particles via the spray route by *in situ* formation and a rapid process. The simplicity of the mechanism can be described as follows: as the aerosol passes through the reactor, solvent evaporation and formation of spherical and compact particles (comprised of all precursor components) occurs sequentially. When the precursor consists of inorganic particles only, spherical particles can be prepared (Fig. 5a; R1). However, when another component (i.e., a CNT catalyst component) is added to the initial precursor, additional phenomena will occur. The catalytic decomposition of ethanol and the CNT growth on the surface of the CNT catalyst happens, which permits the preparation of composite CNT/inorganic particles (Fig. 5a; R2). To the contrary, when no inorganic component is added, the formation of CNT with a thicker diameter can be generated (Fig. 5a; R3) [41].

The results from the above mechanism (in the case of Iskandar et al. [37] and Nandiyanto et al. [43]) are shown in Fig. 5b–e. The formation of dense particles, hairy particles, and CNTs are shown. Aggregated BN particles could be prepared by conducting only

BN nanoparticles in the solvent (Fig. 5b). The addition of catalyst in the initial precursor caused the formation of BN particles with CNT (Fig. 5c). The composite diameter, as well as the CNT population and thickness, could be controlled by a change of the BN/catalyst ratio (Fig. 5d). Finally, when only catalyst existed in the solvent (no BN nanoparticles were placed), CNTs were formed and no aggregated particles existed in the final product (Fig. 5e). To confirm the feasibility of the process in fabricating composite particles, XRD analysis of the prepared particles is shown in Fig. 5f and g. No BN phase change was found during the process, which implies that the current process is reliable for further applications. Moreover, the particle fabrication has the potential for scale-up production due to a short residence time (about 1 s) [37].

3.3. Porous and raspberry-like particles

Technology for the fabrication of honeycomb-patterned material with a well-defined structure has many applications [35]. The improvement in material performance with this pattern has been well-established by several research groups [17]. Many preparation methods, containing pore structures known as the MCM series, the HMS series, the SBA series, etc., have been reported [44]. Although these methods show good utility for industry, several disadvantages are noteworthy: (i) most of these processes have the limitation of producing film material only, which complicates large-scale industrial implementation [45]; (ii) most require and/or produce harmful and difficult-to-handle chemicals (e.g. ammonia as a catalyst), creating conflicts with safety and environmental regulations in industrial applications [46] and necessitating downstream purification processes; (iii) most are specific and require rigid conditions, complicated, and multi-step synthetic procedures, which further complicate the scale-up process; and, (iv) limitations in pore size (less than 5 nm) and particle diameter are common, which can be problematic for many applications [47].

The preparation of porous material in a particle form is promising for industrial application [30]. The particle form can exhibit unique properties [48] and can be re-formed into other types (e.g. film, fiber, packed bed, etc.) [49]. A breakthrough in preparing porous material in particle form has been reported by Nandiyanto et al. [45] which is believed to be the smallest engineered porous particle in existence. It is referred to as the Hiroshima Mesoporous Materials (HMM) series. The control of pore size (from 3 to 20 nm) is possible, as well as in the particle diameter (from several to hundreds of nanometers). The process is amenable to industrial application, although some limitations remain. In overcoming these limitations, the spray-drying method continues to play a key role in the creation of the porous particles.

Combination of the spray method with the use of a template is a common approach to the preparation of porous particles [6]. The principle mechanism involved in the preparation of composite particles (consisting of multi-components as described in the above section) can be used to synthesize this type of particles [35]. However, the additional step is required for creating porous structure in the particles, which typically by eradicating one component from the composite particles is required [50].

Fig. 6 shows the mechanism illustration in creating porous particles and their recent developments. Various porous particles can be seen in this figure. Fig. 6a illustrates the details of the spray method used in porous particle formation. An inorganic material/solution (as the main component) and a template are put into the solvent and used as the precursor. This mixture is then introduced to the atomizer to form droplets. In practical applications, a carrier gas must be utilized to propel the droplets to the solvent removal system (typically using heat treatment), which is described in the above droplet-to-particle step section. The heat treatment can be managed depending on the component proper-

ties (e.g. thermal degradation), which is accomplished by controlling the residence time, the pressure, and the temperature process [5]. Once past the heating system, the composite particles are then put in the template removal process to eradicate the templates, and particles with a porous structure remain. Several common template removal processes have been suggested: (i) heat treatment, and (ii) solvent dissolution via an etching process [5]. Both of the suggested methods have both merits and demerits, which are selected and related to the types of templates and the component properties. However, for industrial applications, heat treatment is typically used as the template removal because the combination between solvent and template removal steps can be approached into one step process [17]. Thus, the total process steps can be minimized.

Selection of the template type is crucial in creating the pore shape and structure [4,30]. Several templates are recommended: salts [51], surfactants [56], polymers [52,53], and colloidal particles [6,17,35,50,54]. Among the templates, an organic compound is typically used because it can be removed easily [6]. In this review, we divided organic templates into two categories. One is an organic liquid/solution (e.g. surfactant, polymer) and the other is an organic particle. The organic liquid/solution is typically chosen due to its convenience and prospect for the creation of a very small pore size. The formation of meso-, wormhole-, and foam-like pore structures is possible depending on the selection of type of organic liquid/solution (Fig. 6b–d). To create particles with a larger pore size, the selection of an organic particle is the best option (Fig. 6e–g). The pore size can be controlled from tens of nanometers [50], which cannot be achieved when using an organic liquid/solution as the template [17]. The pore size and shape can be predicted because the template itself reflects the pore formation [55], which is the main advantage with the use of this type of organic template.

To successfully prepare particles containing a porous structure, the effect of the type of template, main component-to-template ratio, and template concentration and size must be considered [56]. Those parameters manage the pore shape, pore number, and porosity of the prepared particles. In addition to above parameters, the charge [55] of the template is also important. The component attraction–repulsion phenomenon in the precursor, which is resulted from the effect of particle charge selection, is believed to be the main consideration to allow the formation of particles with different morphologies (Fig. 6e and f) [38]. The formation of raspberry-like particles is possible when the main material and the template have opposite charge values (one is positive and the other is negative). This contrast of charges causes an interaction and attraction among the components since they are mixed (prior to spraying), which allows for the phenomenon where one component is coated by other components. When the precursors containing coated particles are spray-dried, aggregations of coated particles form, allowing the formation of raspberry-like particles after the template removal process (Fig. 6e). On the contrary, when the charge values of both components were in the same direction, porous particles were created (Fig. 6f). The pore size that is produced is a reproduction of the initial template particle [6], offering an idea to control pore size through adjustment of the template size. This circumstance also suggested the possibility of a more complicated porous structure material formation, which was then specifically reported by Nandiyanto et al. in designing particles with an art-design pore structure (Fig. 6g) [35]. This material with a unique and multi-size pore structure design could be fabricated by adding multi-size template spheres.

The Okuyama research group has already accomplished much with regard to porous particle preparation. The successful preparation of porous particles has not been limited to only one type of material. The spraying of other inorganic components also has been possible, confirming that this method is reliable and versatile

for the production of various porous particles: SiO₂, ZrO₂, Y₂O₃, Al₂O₃, TiO₂, drugs (hyaluronic acid), etc. [5,6,11,17]. The reliable preparation of many porous particles has been confirmed by the stability of material phase and pattern (as verified by XRD analysis) during the process (drying and template removal process). This group also reported that a change in the size of the template spheres resulted in the control of pore size [17,34,54], which was controllable from several nanometers [50]. These results implied that the success of the spray-drying method is due not only to the choice of a colloidal or nanoparticle sol as the initial precursor, but it is also due to the ability to control the number of pores, pore structure, and pore size [17]. In general, the number of pores, pore structure, and pore size can be controlled by adjusting the concentration of the template and the template size in the initial precursor [35].

3.4. Nanoparticle processing: from conventional spray-drying methods to consideration of additional specific techniques

Particles in the nanometer range (below 100 nm in size) are useful for many applications. Their unique properties distinguish them from bulk materials [57]: (i) their surface structure is unique and different from that of larger crystallites, thus allowing them to alter reactivity or vary crystal chemistry [58]; (ii) in suspension form they usually either sink or float in the liquid. This is because the interaction of the particle surface with the solvent is strong enough to overcome differences in density; (iii) they have unexpected visible properties, especially when they are dispersed into medium, because they are small enough to confine their electrons and produce quantum effects [45]; and, (iv) they have a very high surface-area-to-volume ratio [59].

Based on the special properties of nanoparticles, it is believed that they can lead to the creation of new devices and technologies [60]. This promise is evident by the current rate of production of nanoparticles (i.e. silica and titania), which is 2 million metric tons per year [61]. Furthermore, the annual nanomaterial and nano-catalyst markets are currently estimated to exceed \$3.7 billion [59]. This makes nanoparticles one of the popular artists in science and technology over the past decade [60].

To produce nanoparticles, a traditional method is the basic approach, which progresses through two steps: crystallization fol-

lowed by a milling process to disperse or micronize the prepared crystals. Although the method is feasible for practical uses, it is insufficient due to poor control over particle size and size distribution, particle morphology, and crystallinity.

To address this problem, several developments have been reported to improve the current traditional method, in which the control of reaction rate during the crystal formation seems to be the effective way. For example, the successful preparation of MgF₂ particles with controllable particle size (from nano to submicrometer) and morphology (cubes and spherical shape) has been reported using this technique [48]. Although the preparation of monodispersed particle is possible, shortcomings with regard to impurities and un-reacted components still remain, requiring further processes (e.g. particle functionalization, downstream processing, purification, etc.) that will face a problem with operating costs [2].

3.4.1. Conventional spray-drying method

The spray-drying method can be used as a suitable alternative way to address the problems associated with the traditional method. Its advantages in preparing various particles with a simple process at a high rate of production make it attractive for many applications [30].

According to the literature, the principle of the spray drying method is to produce small-sized particles via atomization and solvent removal [13]. Because a single droplet produces one particle, the size of the droplet and the amount of solvent in the droplet are relative to the final synthesized particle diameter. In short, it is possible to control the outer diameter of the particle, which can easily be achieved by changing the droplet size [62] and adjusting the precursor concentration [63].

The change in droplet size is dependent on the type of atomizer. However, the minimum droplet size that can be generated is about 4.5 μm, which is produced by an ultrasonic atomizer [3]. For this reason, the choice of atomizer is limited in the case of nanoparticle production. To control particle size down to the nanometer range, the change of precursor concentration is the last and the best choice when using the conventional spray-drying method.

The concentration of the main component in the droplet becomes the main option for a change in prepared particle size [50]. When the main component is added to the initial precursor

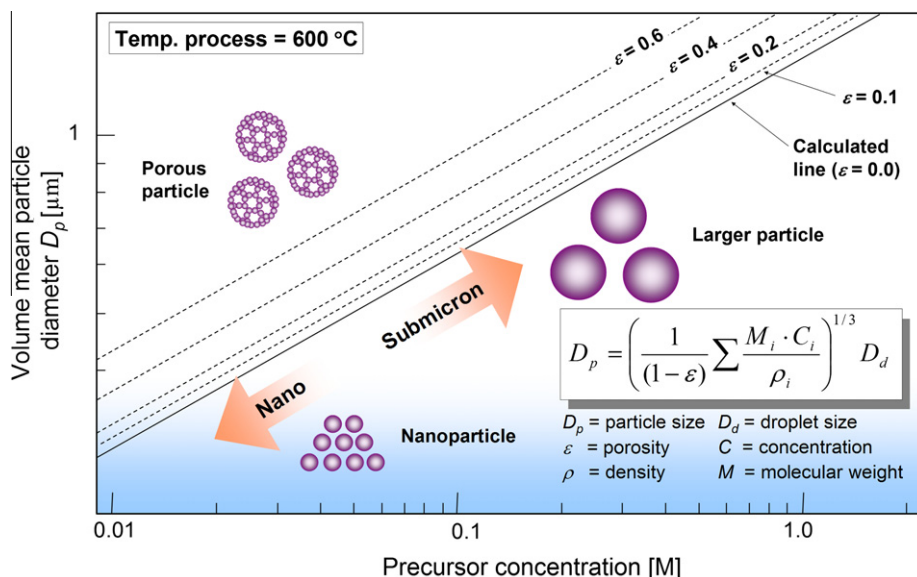


Fig. 7. Prediction of the size of prepared silica particles as a function of the initial precursor concentration.

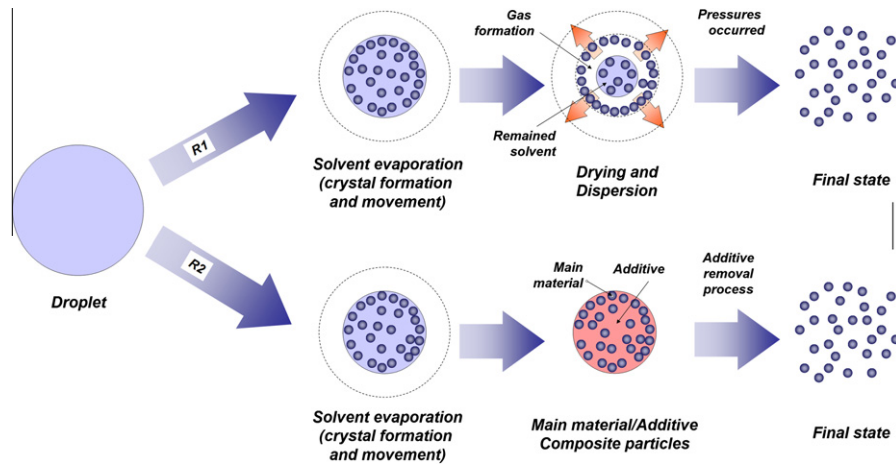


Fig. 8. The nanoparticle formation mechanism using the spray method with the addition of specific techniques.

in small amounts, the concentration ratio of solvent/main component in the droplet should be high. Because the solvent is evaporated during the spray-drying process, the droplets lose most of their volume, allowing the production of small particles. On the contrary, with a high concentration of the main component, after the solvent is removed, the generation of large particles is possible. The correlation between the colloidal concentration and the volume mean diameter of the prepared particles can be calculated using a conventional geometrical droplet calculation, as follows [37]:

$$D_p = \left(\frac{1}{(1-\varepsilon)} \sum \frac{M_i \cdot C_i}{\rho_i} \right)^{1/3} D_d \quad (7)$$

where M_i , C_i , and ρ_i are the molecular weight, the concentration (g/L), and the density (g/L) of component i , respectively. The symbols ε , D_d , and D_p are the porosity of the particle, the volume mean diameter of the droplet, and the volume mean diameter of the final particle, respectively. This correlation proves that the size of generated particles can easily be controlled by changing the initial precursor concentration. The detail of the correlation between precursor concentration and the predicted particle size (using silica as a model material) is represented in Fig. 7.

3.4.2. Additional specific techniques of the spray-drying method

The conventional spray-drying method has shown good ability in fabricating particles on the nanometer scale. A decrease in precursor concentration and a change in droplet size (via selection of atomizer types) are believed to be the main factors affecting the production of nanomaterials. To be industrially relevant, however, the lowering of precursor concentration in order to obtain nanoparticles results in poor production rates [64]. For instance, in a typical initial droplet with a diameter of 5 μm , to obtain a 100 nm particle, the initial precursor concentration must be less than 0.0008%, and such a low precursor concentration is impractical for a scaled-up production [10]. Furthermore, with the conventional spray-drying method, the calculation using Eq. (7) is not as effective in the generation of particles to within several nanometers [62,65].

To overcome the limitations of the prior methodology (in having a high-production rate as well as producing particles in sizes as small as several nanometers), several researchers have reported improvements in the spray-drying method, which can be accomplished through the use of specific conditions. Many techniques have been reported in order to attain such improvements [10].

However, in this review, we have intensively reviewed only two techniques, which are well-known for industrial applications – rapid-solvent evaporation [64,67] and additive-assisted spraying [66].

Fig. 8 illustrates two possible mechanisms for nanoparticle production using these specific techniques. In the first, a micron-sized droplet is produced (after atomization), which then undergoes solvent evaporation. This step is usual for the fabrication of particles using the spray-drying method. However, when an additional improvement is added in the spray drying method, an additional mechanism appears. Fig. 8, route R1, illustrates the mechanism for the rapid-solvent evaporation technique, while Fig. 8, route R2, illustrates the additive-assisted spray method.

Low-pressure-[67] and flame-[64] assisted techniques are typical rapid-solvent evaporation technique models (Fig. 8; R1). The principle of this technique is to use rapid-solvent evaporation to promote fast nucleation and crystal growth inside the droplets. The agglomeration of small particles (formed by fast nucleation and crystal growth) can be retarded due to a short-drying time [68]. Further, an interesting aspect of this method is the formation of an evaporated solvent, or gas evolution, brought about by the thermal reaction and the high-drying rate. This evaporated solvent, or formed gas, will cause pressure inside the droplet system [67], which is the primary promoter of the agglomeration break-up and the dispersion of primary crystals/nanoparticles. The optimization of the properties of the precursor should be considered to enhance the effectiveness of the break-up conditions [69].

In the second route (Fig. 8; R2), nanoparticles can be produced using the additive-assisted spray method. The process is simple, with only a compound added to the precursor prior to spraying. Conventional spray equipment can be used, which is the main advantage of this technique in minimizing capital (equipment) and processing costs. Salts [66], polymers [70], or low boiling-point chemicals [65] are usually used as the additive compounds. The mechanism of this technique can be described as follows. When the multi-components are added to the precursor, they agglomerate inside the spray-dried particles [37]. The additional of additive component to the initial precursor allows the formation of composite particles consisting of the additive and the main components. Although aggregation and/or agglomeration makes all components inseparable, the nano-main components are retained individually inside the composite because the additive prevents agglomeration among them [66]. When the additive components are removed (e.g. solvent dissolution and heat treatment), the nanoparticles can be obtained.

Table 4
Correlation of particle morphology with material properties.

Particle morphology	Precursor	Density	Porosity	Enhancement properties
 Completely spherical dense particle	Solution type (e.g. alkoxide)	$\rho_p = \rho_{app}$	$\varepsilon = 0$	–
 Small rough spherical dense particle	Nanoparticles ($d_{p1} \ll D_d$)	$\rho_p \sim \rho_{app}$	$\varepsilon \sim 0$	Near to normal
 Highly rough spherical dense particle	Nanoparticles ($d_{p1} < D_d$)	$\rho_p < \rho_{app}$	$\varepsilon > 0$	Near to normal
 Hollow particle	Effect of fast evaporation rate	$\rho_p < 0.1 \rho_{app}$	$\varepsilon > 30\%$	Ultra low refractive index
 Doughnut particle	Effect of hydrodynamic	$\rho_p \ll \rho_{app}$	$\varepsilon > 30\%$	High surface area Low refractive index
 Porous particle	Additional template component	0.3 $\rho_{app} < \rho_p < \rho_{app}$	$0 < \varepsilon < 70\%$	Very high surface area Very low refractive index
 Encapsulated particle	Multi component ($d_{p1} > 3d_{p2}$)	$\rho_p \sim \rho_{app}$	$\varepsilon \sim 0$	Protect core material
 Mixed particle	Multi component ($d_{p1} \sim d_{p2}$)	$\rho_p \sim \rho_{app}$	$\varepsilon \sim 0$	Specific properties {e.g. dope material}
 Hairy particle	Multi component ($d_{p1} \sim d_{p2}$) + additional CNT catalyst component	$\rho_p \ll \rho_{app}^*$	$\varepsilon \gg^*$	CNT-related properties

Note: * depend on the CNT population and tube size; ρ_p = particle density; ρ_{app} = densed particle density; ε = porosity; d_p = size of component; d_{p1} = size of component 1; d_{p2} = size of component 2; D_p = size of droplet.

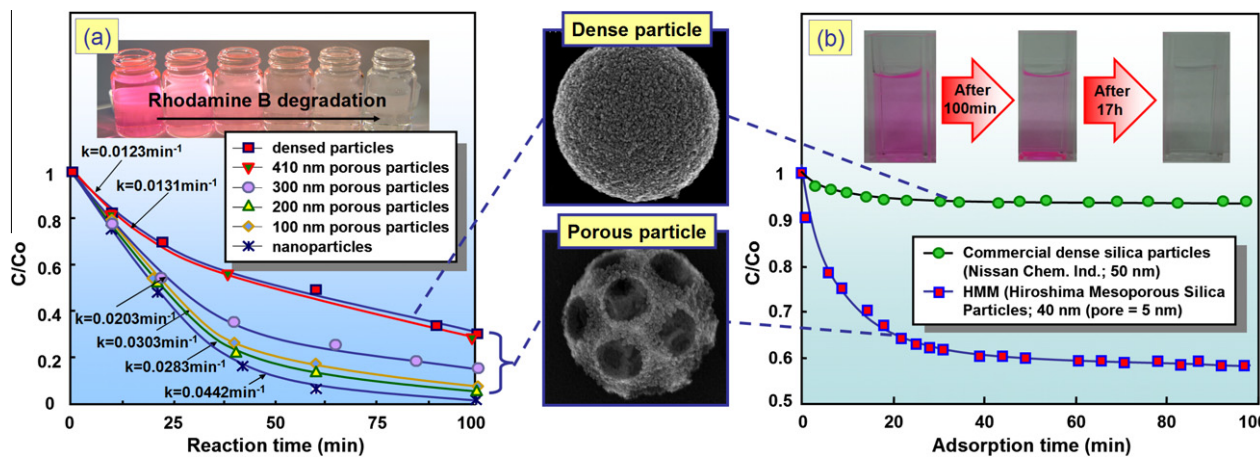


Fig. 9. Effect of particle morphology on catalytic (a) and adsorption ability (b). (a) is a comparison of catalytic performance ability using titania dense and porous particles [6,17], while (b) is a comparison of adsorption performance ability using commercial silica dense particles and the HMM (silica porous particles) [45,47].

Development of the spray-drying method should not be limited to these two techniques. Other advances in development are possible: a pulse combustion-assisted spray-drying method, a filter expansion aerosol generator (FEAG), an electro-spray spray-drying method, etc. [10]. These techniques can be explained simply as follows. (i) The pulse combustion-assisted spray-drying method is used to make droplets break-up and particles burst. This condition gives the synthesized particles a smaller size compared with those produced by conventional spray-drying [71–73]. (ii) The FEAG is a method to make smaller droplets using low-pressure conditions. The difference from the above low-pressure technique is that in FEAG, a filter is utilized as the atomizer. Because the filter has very small pores, the generation of smaller droplets (compared with

those produced by a common atomizer) is possible, allowing the production of nanoparticles in the final product [74]. (iii) Electro-spray is a spray-drying method that applies high voltage to assist in the generation of a small droplet size from a liquid solution that is flowing through a capillary. A controllable droplet size from several nanometers to micrometers is possible, which is one of the main merits of the use of this method [75]. A detailed explanation of the above methods is given elsewhere [10].

4. Particle morphologies – opportunities and potential roles

Particles with engineered features and morphologies are believed to enhance material performance [2]. Coordination of size

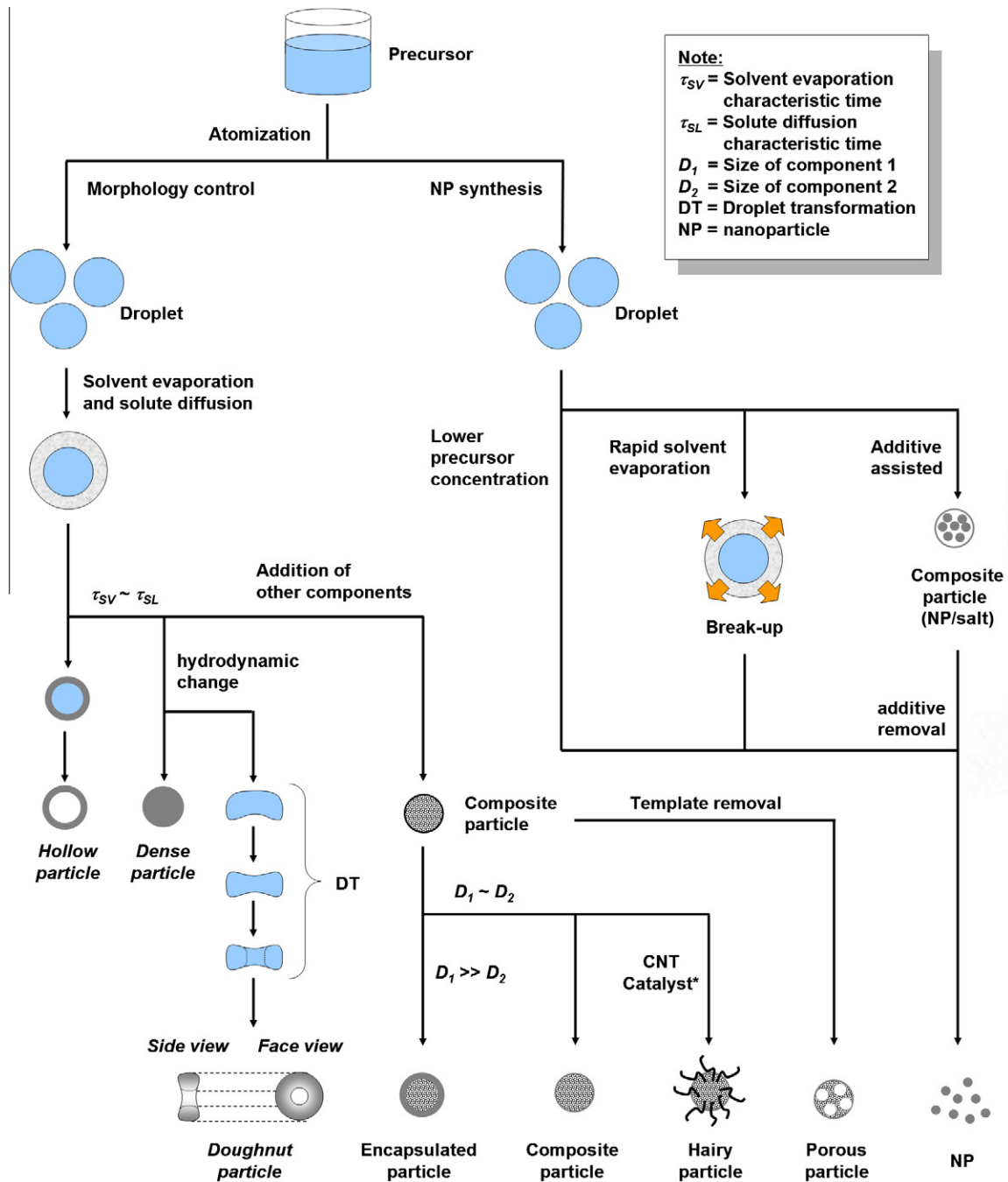


Fig. 10. A summary of the particle morphology preparation using the spray-drying method.

and shape is important in order to gain the optimum particle properties. Exposition of surface performance is one of the advantages of a change in particle morphology. The ratio of active-to-inactive areas becomes a serious concern when expensive precious materials are used for a specific application (e.g., platinum as a catalyst) [59]. Control of particle sizes down to nanometers is the best solution to overcome the problems associated with the use of expensive materials. A nanometer material can obtain the maximum surface area of a material because the value of the inner portion of the particle is relatively lost [59]. Although nanoparticles work well in application, when the particles are too small and some material performance can be compromised or lost [43,59]. Nanoparticles are also difficult to handle in a scale-up production [7]. Their impact on health and the environment has also become a

serious concern [76,77]. The process to re-capture nanoparticles, when they are released into the environment, can be difficult, especially when related to the processing cost and reuse processes [17].

Due to the problems associated with the use of nanoparticles, current technology relies heavily on particles of a larger size (more than submicrometer) [1]. The handling process and the separation of particles within this range is easier giving them greater potential for industrial applications than nanoparticles [7,17]. To garner the properties of nanoparticles, control of particle morphology is a good approach [59]. Chemical–physical performance gained from the management of shape can be predicted and designed [17]. Predictions of particle performance and advantages using various particle morphologies are shown in Table 4.

There are several examples of the use of various particle morphologies. Two examples from the effect of particle morphology on particle performance are represented in Fig. 9. Iskandar et al. reported the effectiveness of the change of morphology on catalytic performance [17]. Porous particles in the submicrometer range have catalytic properties near to that of nanoparticles. Submicrometer porous particles have more utility than nanoparticles for industrial applications because of their cost-effective reuse and recycling processes. This was also verified in a report by Nandiyanto et al. that compared porous particle performance with that of nano and dense particles using other materials [6]. Tsapis et al. reported that the change of particle morphology from dense to hollow is effective for management of material density in the application of aerosol drug delivery [78]. To control particle density and aerodynamics, Iskandar et al. suggested other ways of modifying particles to achieve a porous structure [5]. Lee et al. reported the effect of particle morphology on the change of material density [79]. The effect of various morphologies (i.e., aggregated, porous, and hollow particles) on controlling particle density and porosity was described in detail, both theoretically and experimentally. Okuyama et al. reviewed the change of particle morphology in controlling the material refractive index [30]. The particle refractive index can be controlled to near that of the ideal refractive index material (e.g. air) by changing the particle shape [80]. Success in changing particle morphology is not exclusively in the material density, surface area, and refractive index. Widiyastuti et al. reported the effectiveness of the use of porous particles, which exhibited greater PL intensity, quantum efficiency, and red-emission compared with non-porous particles [81].

5. Summary

Critical issues, associated with the development of the aerosol-assisted self-assembly technique to obtain effective strategies in designing particle morphology, have been discussed. The spray method, as the representative of this technique, has been verified for the production of particles with various features and morphologies. The types and the concentrations of precursors, the selection of process conditions, and the addition of supporting materials all play significant roles in the production of particles with various sizes and morphologies.

To comprehend the above description of particle morphology, Fig. 10 shows the various particle morphologies prepared using the spray method. The effectiveness of this method in controlling particle morphologies that include dense, hollow, encapsulated, hairy, and doughnut forms has been described. An explanation of the various morphologies can be simplified as follows:

- (i) The spherical particles are basically prepared using the spray method because the particles are produced from the droplets with a spherical shape, and the most stable shape for a droplet is the spherical form.
- (ii) The particles with doughnut and hollow shapes can be prepared by changing the process conditions (e.g., flow rate, temperature process, addition of surfactant).
- (iii) The production of particles with a multi-component is possible when multi-components are added to the initial precursor. Well-mixed component particles can be created when the component fractions (i.e., size) are almost the same, while the possibility of the particle encapsulation phenomenon can be prepared when the component fractions are different.
- (iv) The hairy particle can be produced when the specific material (i.e., a CNT catalyst) is added to the precursor.
- (v) The particle with porous structures can be formed when the template component is added to the precursor.

The various morphologies of particles exhibit many potential applications for their uses in future technology. Enhancement of particle performance can be achieved by a change in particle morphology. We believe this report contributes new information to the fields of chemical, material, environmental, and medical engineering because the method that we reviewed has shown that broad application can be born from the management of particle morphology. Finally, size- and morphological-controllable synthesis of particles is of both great significance and challenge, and need to be further explored.

Acknowledgements

A scholarship provided by the Japanese Ministry of Education, Science, Sports, and Culture (MEXT) for A.B.D.N. is gratefully acknowledged. We also thank the Hosokawa Micron Foundation for providing a research allowance to ABDN. We thank Tuswadi of the Faculty of IDEC of Hiroshima University for preparing materials and assistance in this report. We are also grateful to Dr. Ferry Iskandar of the Department of Physics of Institut Teknologi Bandung (ITB) and Dr. Chris Hogan of the Department of Mechanical Engineering of University of Minnesota for their help and for their consultation.

References

- [1] W.H. Suh, A.R. Jang, Y.H. Suh, K.S. Suslick, Porous, hollow, and ball-in-ball metal oxide microspheres: preparation, endocytosis, and cytotoxicity, *Advanced Materials* 18 (14) (2006) 1832–1837.
- [2] H.-K. Chan, Dry powder aerosol drug delivery – opportunities for colloid and surface scientists, *Colloids and Surfaces A: Physicochemical and Engineering Aspects* 284–285 (2006) 50–55.
- [3] F. Iskandar, Nanoparticle processing for optical applications – a review, *Advanced Powder Technology* 20 (4) (2009) 283–292.
- [4] J.H. Bang, K.S. Suslick, Applications of ultrasound to the synthesis of nanostructured materials, *Advanced Materials* 22 (10) (2010) 1039–1059.
- [5] F. Iskandar, A.B.D. Nandiyanto, W. Widiyastuti, L.S. Young, K. Okuyama, L. Gradon, Production of morphology-controllable porous hyaluronic acid particles using a spray-drying method, *Acta Biomaterialia* 5 (4) (2009) 1027–1034.
- [6] A.B.D. Nandiyanto, F. Iskandar, K. Okuyama, Macroporous anatase titania particle: aerosol self-assembly fabrication with photocatalytic performance, *Chemical Engineering Journal* 152 (1) (2009) 293–296.
- [7] F. Iskandar, I.W. Lengggoro, B. Xia, K. Okuyama, Functional nanostructured silica powders derived from colloidal suspensions by sol spraying, *Journal of Nanoparticle Research* 3 (4) (2001) 263–270.
- [8] I. Zbicinski, A. Delag, C. Strumillo, J. Adamiec, Advanced experimental analysis of drying kinetics in spray drying, *Chemical Engineering Journal* 86 (1–2) (2002) 207–216.
- [9] S. Wang, T. Langrish, A review of process simulations and the use of additives in spray drying, *Food Research International* 42 (1) (2009) 13–25.
- [10] K. Okuyama, I.W. Lengggoro, Preparation of nanoparticles via spray route, *Chemical Engineering Science* 58 (3–6) (2003) 537–547.
- [11] M. Abdullah, F. Iskandar, S. Shibamoto, T. Ogi, K. Okuyama, Preparation of oxide particles with ordered macropores by colloidal templating and spray pyrolysis, *Acta Materialia* 52 (17) (2004) 5151–5156.
- [12] K. Leong, Morphological control of particles generated from the evaporation of solution droplets: experiment, *Journal of Aerosol Science* 18 (5) (1987) 525–552.
- [13] K. Masters, *Spray drying handbook*, Longman Scientific & Technical, London, 1994.
- [14] A.J. Hewitt, Droplet size spectra produced by air-assisted atomizers, *Journal of Aerosol Science* 24 (2) (1993) 155–162.
- [15] W.N. Wang, A. Purwanto, I.W. Lengggoro, K. Okuyama, H. Chang, H.D. Jang, Investigation on the correlations between droplet and particle size distribution in ultrasonic spray pyrolysis, *Industrial & Engineering Chemistry Research* 47 (5) (2008) 1650–1659.
- [16] W. Widiyastuti, S.Y. Lee, F. Iskandar, K. Okuyama, Sintering behavior of spherical aggregated nanoparticles prepared by spraying colloidal precursor in a heated flow, *Advanced Powder Technology* 20 (4) (2009) 318–326.
- [17] F. Iskandar, A.B.D. Nandiyanto, K.M. Yun, C.J. Hogan, K. Okuyama, P. Biswas, Enhanced photocatalytic performance of brookite TiO₂ macroporous particles prepared by spray drying with colloidal templating, *Advanced materials* 19 (10) (2007) 1408–1412.
- [18] Z. Yu, T.L. Rogers, J. Hu, K.P. Johnston, R.O. Williams 3rd, Preparation and characterization of microparticles containing peptide produced by a novel process: spray freezing into liquid, *European Journal of Pharmaceutical Biopharmaceutics* 54 (2) (2002) 221–228.

- [19] R. Vehring, W.R. Foss, D. Lechuga-Ballesteros, Particle formation in spray drying, *Journal of Aerosol Science* 38 (7) (2007) 728–746.
- [20] R. Vehring, Pharmaceutical particle engineering via spray drying, *Pharmaceutical Research* 25 (5) (2008) 999–1022.
- [21] G.A.E. Godsave, In studies of the combustion of drops in a fuel spray: the burning of single drops of fuel, Fourth Symposium (International) on combustion, Baltimore, US, 1953, Williams and Wilkins, Baltimore, US, 1953, pp. 818–830.
- [22] H. Krier, Ja. Wronkiew, Combustion of single drops of fuel, *Combustion and Flame* 18 (2) (1972) 159–166.
- [23] W.H. Finlay, *The Mechanics of Inhaled Pharmaceutical Aerosols*, Academic Press, San Diego, 2001.
- [24] M. Rhodes, *Introduction to Particle Technology*, second ed., John Wiley & Sons Ltd., West Sussex, England, 2008.
- [25] available from <http://www.env.go.jp/earth/coop/coop/materials/01-apctme/01-apctme-0706.pdf>.
- [26] L. Svarovsky, *Solid-gas separation*, Elsevier Scientific Publishing, New York, 1981.
- [27] L. Svarovsky, *Solid-gas separation*, in: M.J. Rhodes (Ed.), *Principles of Powder Technology*, John Wiley & Sons, Ltd., Chichester, 1990, pp. 171–192.
- [28] R.H. Perry, D.W. Green, J.O. Maloney, *Perry's Chemical Engineers' Handbook*, McGraw-Hill, New York, 1997.
- [29] W. Widiyastuti, W.N. Wang, I.W. Lenggono, F. Iskandar, K. Okuyama, Simulation and experimental study of spray pyrolysis of polydispersed droplets, *Journal of Materials Research* 22 (7) (2007) 1888–1898.
- [30] K. Okuyama, M. Abdullah, I.W. Lenggono, F. Iskandar, Preparation of functional nanostructured particles by spray drying, *Advanced Powder Technology* 17 (6) (2006) 587–611.
- [31] H.W. Chang, K. Okuyama, Optical properties of dense and porous spheroids consisting of primary silica nanoparticles, *Journal of Aerosol Science* 33 (12) (2002) 1701–1720.
- [32] F. Iskandar, L. Gradon, K. Okuyama, Control of the morphology of nanostructured particles prepared by the spray drying of a nanoparticle sol, *Journal of Colloid and Interface Science* 265 (2) (2003) 296–303.
- [33] A. Gharsallaoui, G.J. Roudaut, O. Chambin, A. Voilley, R. Saurel, Applications of spray-drying in microencapsulation of food ingredients: an overview, *Food Research International* 40 (9) (2007) 1107–1121.
- [34] L. Gradon, S. Janeczko, M. Abdullah, F. Iskandar, K. Okuyama, Self-organization kinetics of mesoporous nanostructured particles, *Aiche Journal* 50 (10) (2004) 2583–2593.
- [35] A.B.D. Nandiyanto, N. Hagura, F. Iskandar, K. Okuyama, Design of a highly ordered and uniform porous structure with multisized pores in film and particle forms using a template-driven self-assembly technique, *Acta Materialia* 58 (1) (2010) 282–289.
- [36] F. Iskandar, H.W. Chang, K. Okuyama, Preparation of microencapsulated powders by an aerosol spray method and their optical properties, *Advanced Powder Technology* 14 (3) (2003) 349–367.
- [37] F. Iskandar, S.G. Kim, A.B.D. Nandiyanto, Y. Kaihatsu, T. Ogi, K. Okuyama, Direct synthesis of hBN/MWCNT composite particles using spray pyrolysis, *Journal of Alloys and Compounds* 471 (1–2) (2009) 166–171.
- [38] N. Hagura, A.B.D. Nandiyanto, F. Iskandar, K. Okuyama, A role of template surface charge in the preparation of porous and hollow particles using spray-drying, *Chemistry Letters* 38 (11) (2009) 1076–1077.
- [39] M. Inagaki, K. Kaneko, T. Nishizawa, Nanocarbons – recent research in Japan, *Carbon* 42 (8–9) (2004) 1401–1417.
- [40] S.R.C. Vivechand, L.M. Cele, F.L. Deepak, A.R. Raju, A. Govindaraj, Carbon nanotubes by nebulized spray pyrolysis, *Chemical Physics Letters* 386 (4–6) (2004) 313–318.
- [41] L.F. Su, J.N. Wang, F. Yu, Z.M. Sheng, H. Chang, C.H. Pak, Continuous production of single-wall carbon nanotubes by spray pyrolysis of alcohol with dissolved ferrocene, *Chemical Physics Letters* 420 (4–6) (2006) 421–425.
- [42] M. Bottini, L. Tautz, H. Huynh, E. Monosov, N. Bottini, M.I. Dawson, S. Bellucci, T. Mustelin, Covalent decoration of multi-walled carbon nanotubes with silica nanoparticles, *Chemical Communications* 6 (2005) 758–760.
- [43] A.B.D. Nandiyanto, Y. Kaihatsu, F. Iskandar, K. Okuyama, Rapid synthesis of a BN/CNT composite particle via spray routes using ferrocene/ethanol as a catalyst/carbon source, *Materials Letters* 63 (21) (2009) 1847–1850.
- [44] A. Taguchi, F. Schh, Ordered mesoporous materials in catalysis, *Microporous and Mesoporous Materials* 77 (1) (2005) 1–45.
- [45] A.B.D. Nandiyanto, S.G. Kim, F. Iskandar, K. Okuyama, Synthesis of spherical mesoporous silica nanoparticles with nanometer-size controllable pores and outer diameters, *Microporous and Mesoporous Materials* 120 (3) (2009) 447–453.
- [46] S.V. Krupa, Effects of atmospheric ammonia (NH₃) on terrestrial vegetation: a review, *Environmental Pollution* 124 (2) (2003) 179–221.
- [47] A.B.D. Nandiyanto, Y. Kaihatsu, F. Iskandar, K. Okuyama, Controllable mesopore-size and outer diameter of silica nanoparticles prepared by a novel water/oil-phase technique, in: *Materials Research Society Symposium Proceedings, MRS Fall Meeting 2009*, vol. 1220, Boston, 2009, pp. 11–17.
- [48] A.B.D. Nandiyanto, F. Iskandar, T. Ogi, K. Okuyama, Nanometer to submicrometer magnesium fluoride particles with controllable morphology, *Langmuir* 26 (14) (2010) 12260–12266.
- [49] Y. Endo, C.L.Y. Ngan, A.B.D. Nandiyanto, F. Iskandar, K. Okuyama, Analysis of fluid permeation through a particle-packed layer using an electric resistance network as an analogy, *Powder Technology* 191 (1–2) (2009) 39–46.
- [50] A.B.D. Nandiyanto, F. Iskandar, K. Okuyama, Nanosized polymer particle-facilitated preparation of mesoporous silica particles using a spray method, *Chemistry Letters* 37 (10) (2008) 1040–1041.
- [51] A.K. Peterson, D.G. Morgan, S.E. Skrabalak, Aerosol synthesis of porous particles using simple salts as a pore template, *Langmuir* (2010) 60–103.
- [52] T. Kimura, K. Kato, Y. Yamauchi, Temperature-controlled and aerosol-assisted synthesis of aluminium organophosphate spherical particles with uniform mesopores, *Chemical Communications* 33 (2009) 4938–4940.
- [53] B. Nagaraja, H. Abimanyu, K. Jung, K. Yoo, Novel method for the preparation of mesoporous BaSO₄ material with thermal stability by spray pyrolysis, *Bulletin Korean Chemical Society* 29 (5) (2008) 1007–1012.
- [54] F. Iskandar, Mikrajuddin, K. Okuyama, In situ production of spherical silica particles containing self-organized mesopores, *Nano Letters* 1 (5) (2001) 231–234.
- [55] X.L. Ji, Q.Y. Hu, J.E. Hampsey, X.P. Qiu, L.X. Gao, J.B. He, Y.F. Lu, Synthesis and characterization of functionalized mesoporous silica by aerosol-assisted self-assembly, *Chemistry of Materials* 18 (9) (2006) 2265–2274.
- [56] Y.F. Lu, H.Y. Fan, A. Stump, T.L. Ward, T. Rieker, C.J. Brinker, Aerosol-assisted self-assembly of mesostructured spherical nanoparticles, *Nature* 398 (6724) (1999) 223–226.
- [57] C.P. Poole, F.J. Owens, *Introduction to Nanotechnology*, Wiley-Interscience, 2003.
- [58] G.A. Waychunas, C.S. Kim, J.F. Banfield, Nanoparticulate iron oxide minerals in soils and sediments: unique properties and contaminant scavenging mechanisms, *Journal of Nanoparticle Research* 7 (4) (2005) 409–433.
- [59] B. Zhou, R. Balee, R. Groenendaal, Nanoparticle and nanostructure catalysts: technologies and markets, *Nanotechnology Law and Business* 2 (3) (2003) 222–229.
- [60] C. Rao, New developments of nanomaterials, *Journal of Materials Chemistry Letters* 14 (2004) E4.
- [61] R.N. Grass, W.J. Stark, Flame spray synthesis under a non-oxidizing atmosphere: preparation of metallic bismuth nanoparticles and nanocrystalline bulk bismuth metal, *Journal of Nanoparticle Research* 8 (5) (2006) 729–736.
- [62] L. Amirav, A. Amirav, E. Lifshitz, A spray-based method for the production of semiconductor nanocrystals, *Journal of Physical Chemistry B* 109 (20) (2005) 9857–9860.
- [63] F. Iskandar, I.W. Lenggono, T.O. Kim, N. Nakao, M. Shimada, K. Okuyama, Fabrication and characterization of SiO₂ particles generated by spray method for standards aerosol, *Journal of Chemical Engineering of Japan* 34 (10) (2001) 1285–1292.
- [64] S.A. Song, K.Y. Jung, S.B. Park, Preparation of Y₂O₃ particles by flame spray pyrolysis with emulsion, *Langmuir* 25 (6) (2009) 3402–3406.
- [65] Y.T. Didenko, K.S. Suslick, Chemical aerosol flow synthesis of semiconductor nanoparticles, *Journal of the American Chemical Society* 127 (35) (2005) 12196–12197.
- [66] B. Xia, I.W. Lenggono, K. Okuyama, Synthesis of CeO₂ nanoparticles by salt-assisted ultrasonic aerosol decomposition, *Journal of Materials Chemistry* 11 (12) (2001) 2925–2927.
- [67] W.N. Wang, I.W. Lenggono, Y. Terashi, T.O. Kim, K. Okuyama, One-step synthesis of titanium oxide nanoparticles by spray pyrolysis of organic precursors, *Materials Science and Engineering B-Solid State Materials for Advanced Technology* 123 (3) (2005) 194–202.
- [68] Y.C. Kang, S.B. Park, Y.W. Kang, Preparation of high-surface-area nanophase particles by low-pressure spray-pyrolysis, *Nanostructured Materials* 5 (7–8) (1995) 777–791.
- [69] R. Strobel, A. Baiker, S.E. Pratsinis, Aerosol flame synthesis of catalysts, *Advanced Powder Technology* 17 (5) (2006) 457–480.
- [70] S.H. Kim, B.Y.H. Liu, M.R. Zachariah, Synthesis of nanoporous metal oxide particles by a new inorganic matrix spray pyrolysis method, *Chemistry of Materials* 14 (7) (2002) 2889–2899.
- [71] W. Widiyastuti, W.N. Wang, A. Purwanto, I.W. Lenggono, K. Okuyama, A pulse combustion-spray pyrolysis process for the preparation of nano- and submicrometer-sized oxide particles, *Journal of the American Ceramic Society* 90 (12) (2007) 3779–3785.
- [72] P.S. Kuts, P.V. Akulich, N.N. Grinchik, C. Strumillo, I. Zbicinski, E.F. Nogotov, Modeling of gas dynamics in a pulse combustion chamber to predict initial drying process parameters, *Chemical Engineering Journal* 86 (1–2) (2002) 25–31.
- [73] Y. Watanabe, T. Ikoma, A. Monkawa, Y. Suetsugu, H. Yamada, J. Tanaka, Y. Moriyoshi, Fabrication of transparent hydroxyapatite sintered body with high crystal orientation by pulse electric current sintering, *Journal of the American Ceramic Society* 88 (1) (2005) 243–245.
- [74] Y.C. Kang, S.B. Park, Preparation of nanometre size oxide particles using filter expansion aerosol generator, *Journal of Materials Science* 31 (9) (1996) 2409–2416.
- [75] I.W. Lenggono, K. Okuyama, J.F. de la Mora, N. Tohge, Preparation of ZnS nanoparticles by electrospray pyrolysis, *Journal of Aerosol Science* 31 (1) (2000) 121–136.
- [76] C.W. Lam, J.T. James, R. McCluskey, S. Arepalli, R.L. Hunter, A review of carbon nanotube toxicity and assessment of potential occupational and environmental health risks, *Critical reviews in toxicology* 36 (3) (2006) 189–217.
- [77] R.J. Aitken, M.Q. Chaudhry, A.B.A. Boxall, M. Hull, Manufacture and use of nanomaterials: current status in the UK and global trends, *Society Occupational Medicine* 56 (2006) 300–306.

- [78] N. Tzapis, D. Bennett, B. Jackson, D.A. Weitz, D.A. Edwards, Trojan particles: large porous carriers of nanoparticles for drug delivery, *Proceedings of the National Academy of Sciences of the United States of America* 99 (19) (2002) 12001–12005.
- [79] S.Y. Lee, W. Widiyastuti, N. Tajima, F. Iskandar, K. Okuyama, Measurement of the effective density of both spherical aggregated and ordered porous aerosol particles using mobility- and mass-analyzers, *Aerosol Science and Technology* 43 (2) (2009) 136–144.
- [80] F. Iskandar, M. Abdullah, H. Yoden, K. Okuyama, Optical band gap and ultralow dielectric constant materials prepared by a simple dip coating process, *Journal of Applied Physics* 93 (2003) 9327–9342.
- [81] W. Widiyastuti, T. Minami, W.N. Wang, F. Iskandar, K. Okuyama, Photoluminescence characteristics of macroporous Eu-doped yttrium oxide particles prepared by spray pyrolysis, *Japanese Journal of Applied Physics* 48 (3) (2009) 0320011–0320015.
- [82] G.E. Lorenzetto, A.H. Lefebvre, Measurements of Drop Size on a Plain-Jet Airblast Atomizer, *AIAA Journal* 15 (7) (1977) 1006–1010.
- [83] A.K. Jasuja, Plain-jet airblast atomization of alternative liquid petroleum fuels under high ambient air pressure conditions. in: *International Gas Turbine Conference and Exhibit 27th*, American Society of Mechanical Engineers, pp. 7. London, England (1982).
- [84] W.H. Walton, W.C. Prewett, The production of sprays and mists of uniform drop size by means of spinning disc type sprayers, *Proceedings of the Physical Society. Section A* 62 (354) (1949) 399.
- [85] Y. Oyama, M. Eguti, K. Endou, On the centrifugal disc atomisation and studies on the atomisation of water droplets, *Kagaku Kogaku* 17 (1953) 269.
- [86] R.P. Fraser, E.P. Eisenklam, N. Dombrowski, Liquid atomization in chemical engineering: part 2. Rotary atomizers, *British Chemical Engineering* (1957) 496–501.
- [87] D.J. Ryley, Analysis of a polydisperse aqueous spray from a high-speed spinning disk atomizer, *British Journal of Applied Physics* 10 (4) (1959) 180–186.
- [88] N. Dombrowski, T.L. Lloyd, Atomisation of liquids by spinning cups, *Chemical Engineering Journal* 8 (1974) 63–81.
- [89] A. Kayano, T. Kamiya, Calculation of the mean size of droplets purged from the rotating disc., in: *Proceeding 1st International Conference on Liquid Atomization and Spray Systems*, Fuel Society of Japan, pp. 133–143. Tokyo, Japan (1978).
- [90] Y. Tanasawa, Y. Miyasaka, M. Umehara, Effect of shape of rotating disks and cups on liquid atomisation, in: *Proc. 1st International Conference on Liquid Atomisation and Spray Systems*, Fuel Society of Japan, pp. 165–172, Tokyo, Japan (1978).
- [91] A.R. Frost, Rotary Atomization in the Ligament Formation Mode, *Journal of Agricultural Engineering Research* 26 (1) (1981) 63–78.
- [92] C.S. Parkin, H.A. Siddiqui, Measurement of drop spectra from rotary cage aerial atomizers, *Crop Protection* 9 (1) (1990) 33–38.
- [93] R.J. Lang, Ultrasonic atomization of liquids, *Journal of the Acoustical Society of America* 34 (1) (1962) 6–8.
- [94] T. Mochida, in: *Proc. ICLASS-78* (1978) 193.
- [95] R. Rajan, A.B. Pandit, Correlations to predict droplet size in ultrasonic atomisation, *Ultrasonics* 39 (4) (2001) 235–255.
- [96] Y.C. Kang, S. Bin Park, Morphology of $(YxGd1-x)BO_3$: Eu phosphor particles prepared by spray pyrolysis from aqueous and colloidal solutions, *Japanese Journal of Applied Physics Part 2-Letters* 38 (12B) (1999) L1541–L1543.
- [97] Y.L. Song, S.C. Tsai, C.Y. Chen, T.K. Tseng, C.S. Tsai, J.W. Chen, Y.D. Yao, Ultrasonic spray pyrolysis for synthesis of spherical zirconia particles, *Journal of the American Ceramic Society* 87 (10) (2004) 1864–1871.
- [98] F. Gao, Z. Tang, J. Xue, Preparation and characterization of nano-particle $LiFePO_4$ and $LiFePO_4/C$ by spray-drying and post-annealing method, *Electrochimica Acta* 53 (4) (2007) 1939–1944.
- [99] D. Sen, S. Mazumder, J.S. Melo, A. Khan, S. Bhattacharya, S.F. D'Souza, Evaporation Driven Self-Assembly of a Colloidal Dispersion during Spray Drying: Volume Fraction Dependent Morphological Transition, *Langmuir* 25 (12) (2009) 6690–6695.
- [100] R.X. Sun, Y.P. Lu, K.Z. Chen, Preparation and characterization of hollow hydroxyapatite microspheres by spray drying method, *Materials Science & Engineering C-Biomimetic and Supramolecular Systems* 29 (4) (2009) 1088–1092.
- [101] X.H. Du, Z.W. Jiang, X.Y. Meng, Z. Wang, H.O. Yu, M.Y. Li, T. Tang, Syntheses of opened hollow clay microspheres through a spray-drying approach and their derivative clay/carbon nanotubes composites, *Journal of Physical Chemistry C* 112 (17) (2008) 6638–6642.
- [102] X.L. Yu, S.J. Ding, Z.K. Meng, J.G. Liu, X.Z. Qu, Y.F. Lu, Z.Z. Yang, Aerosol assisted synthesis of silica/phenolic resin composite mesoporous hollow spheres, *Colloid and Polymer Science* 286 (12) (2008) 1361–1368.
- [103] H.S. Kang, Y.C. Kang, H.D. Park, Y.G. Shul, Morphology of particles prepared by spray pyrolysis from organic precursor solution, *Materials Letters* 57 (7) (2003) 1288–1294.
- [104] L. Pawlowski, *The Science and Engineering of Thermal Spray Coatings*, second edition ed., John Wiley & Sons, West Sussex, England, 2008.
- [105] S. Ersus, U. Yurdagel, Microencapsulation of anthocyanin pigments of black carrot (*Daucuscarota L.*) by spray drier, *Journal of Food Engineering* 80 (3) (2007) 805–812.
- [106] B. Shu, W.L. Yu, Y.P. Zhao, X.Y. Liu, Study on microencapsulation of lycopene by spray-drying, *Journal of Food Engineering* 76 (4) (2006) 664–669.
- [107] H. Isobe, K. Kaneko, Porous silica particles prepared from silicon tetrachloride using ultrasonic spray method, *Journal of Colloid and Interface Science* 212 (2) (1999) 234–241.
- [108] J.H. Kim, K.Y. Jung, K.Y. Park, S.B. Cho, Characterization of mesoporous alumina particles prepared by spray pyrolysis of $Al(NO_3)_3$ center dot $9H_2O$ precursor: Effect of CTAB and urea, *Microporous and Mesoporous Materials* 128 (1–3) (2010) 85–90.
- [109] S. Skrabalak, K. Suslick, Porous carbon powders prepared by ultrasonic spray pyrolysis, *J. Am. Chem. Soc* 128 (39) (2006) 12642–12643.
- [110] I.W. Lenggoro, Y. Itoh, K. Okuyama, T.O. Kim, Nanoparticles of a doped oxide phosphor prepared by direct-spray pyrolysis, *Journal of Materials Research* 19 (12) (2004) 3534–3539.
- [111] H.S. Kang, Y.C. Kang, H.Y. Koo, S.H. Ju, D.Y. Kim, S.K. Hong, J.R. Sohn, K.Y. Jung, S.B. Park, Nano-sized ceria particles prepared by spray pyrolysis using polymeric precursor solution, *Materials Science and Engineering B-Solid State Materials for Advanced Technology* 127 (2–3) (2006) 99–104.
- [112] R. Mueller, L. Mädler, S. Pratsinis, Nanoparticle synthesis at high production rates by flame spray pyrolysis, *Chemical Engineering Science* 58 (10) (2003) 1969–1976.
- [113] A. Purwanto, W.N. Wang, T. Ogi, I.W. Lenggoro, E. Tanabe, K. Okuyama, High luminance YAG : Ce nanoparticles fabricated from urea added aqueous precursor by flame process, *Journal of Alloys and Compounds* 463 (1–2) (2008) 350–357.